metals

MDPI

Review

Plant-Based Corrosion Inhibitors for Reinforced Concrete Under Chloride Attack: Advances, Mechanisms, and Prospects

Mingyuan Xiong [1], Changshi Huang [1], Guowei Wang [1], Xiaocheng Zhou [1,*] and Dan Song [1,2,3,*]

[1] College of Materials Science and Engineering, Hohai University, Changzhou 213200, China
[2] Jiangsu Provincial Engineering Research Center for Structure-Function Integrated Metallic Materials for Harsh Environments, Hohai University, Changzhou 213200, China
[3] Innovation Center for Critical Materials in Hydraulic Infrastructure Safety and Water Environment Restoration, Hohai University, Changzhou 213200, China
* Correspondence: zhxc512@126.com (X.Z.); songdancharls@hhu.edu.cn (D.S.)

Abstract

Chloride-induced steel corrosion is one of the major causes of durability degradation in reinforced concrete (RC) structures. Conventional inhibitors have inherent drawbacks in environmental safety, long-term stability, and cement compatibility. Plant extracts, featuring renewability, biodegradability, and abundant bioactive components, have emerged as promising green corrosion inhibitors. This review summarizes the categories, inhibition mechanisms, and evaluation methods of plant-based inhibitors, and discusses multi-scale characterization and computational techniques for mechanism research. A conceptual *Ginkgo biloba* extract (EGb)-LDH strategy is discussed as a possible future route for plant-based inhibitor delivery, but its chloride-responsive release and corrosion-protection performance remain to be experimentally verified.

Keywords: green corrosion inhibitors; reinforced concrete; plant extracts; *Ginkgo biloba* extract (EGb); layered double hydroxide (LDH)

1. Introduction

Reinforced concrete (RC) is one of the most widely adopted structural forms in modern construction and infrastructure, owing to its favorable mechanical performance, durability, low cost, and flexible constructability [1]. However, steel reinforcement corrosion—one of the primary causes of RC durability degradation—causes estimated hundreds of billions of dollars in annual global economic losses and drastically reduces structural service life [2]. Chloride from marine atmospheres and deicing salts is a primary cause of steel corrosion in coastal and cold regions: chloride ions penetrate concrete pores and microcracks to destroy the steel passive film, and the resultant expansion of corrosion products induces concrete cracking and spalling, severely impairing structural load capacity [3–5]. In China, the boom of major infrastructure under national strategies has made chloride-induced corrosion cracking increasingly prominent, rendering corrosion mitigation a key technical challenge for durable civil infrastructure [4,6].

Current strategies to mitigate steel corrosion include enhancing concrete compactness, applying external protective barriers, using corrosion-resistant rebars, and incorporating corrosion inhibitors [7–10]. Corrosion inhibitors are widely applied for their convenient construction, cost-effectiveness, and high efficacy [11,12]. Nevertheless, conventional inorganic inhibitors (e.g., sodium nitrite, chromates) are highly toxic and ecologically harmful, and have been restricted by EU REACH and Chinese regulations [13]; traditional

Academic Editor: Branimir N. Grgur

Received: 25 July 2026
Revised: 27 August 2026
Accepted: 1 September 2026
Published: 3 September 2026

organic inhibitors also suffer from poor biodegradability and high production energy consumption. Driven by global carbon neutrality goals, developing green, efficient, and sustainable inhibitors has become a key research focus [14,15].

Plant-based inhibitors have received increasing attention in recent years, mainly because of their renewable sources, biodegradability, and potentially lower environmental burden [16]. Plant secondary metabolites, including alkaloids, flavonoids, and other phenolic compounds, contain N/O/S/P heteroatoms and π-conjugated systems, forming dense protective films on steel surfaces via physical and chemical adsorption [17]. Active ingredients derived from agroforestry byproducts have demonstrated promising corrosion-inhibition performance in both simulated pore solutions and concrete systems. Under certain laboratory conditions, some reported inhibition efficiencies exceed 90%, which is comparable to, or even higher than, that of conventional nitrite-based inhibitors in the same test environments [18–21]. With the continuous advancement of scientific research, plant-based corrosion inhibitors are expected to show strong application potential in civil engineering and industrial corrosion protection, offering a sustainable alternative for corrosion protection in reinforced concrete infrastructure [21].

Nevertheless, several key bottlenecks still restrict the further popularization and engineering application of plant-based corrosion inhibitors [22,23]: the lack of standardized quantitative characterization criteria, which leads to considerable variation in reported optimal dosages across studies; progressive performance degradation during long-term exposure in concrete environments; insufficient understanding of multi-component synergistic effects and interfacial adsorption configurations; and the reliance on a single passive protection mode, which is difficult to reconcile with the intelligent and on-demand regulation requirements of modern durable concrete structures.

This paper reviews recent progress in plant-based corrosion inhibitors for RC structures under chloride attack with a focus on enhancement strategies, performance evaluation, active components, inhibition efficiency, and interfacial mechanisms. Key challenges and future directions are also discussed to provide theoretical guidance for the development of high-performance plant-based inhibitors and support the long-term durability of RC structures in harsh environments.

2. Review Methodology and Literature-Screening Strategy

A structured literature search was conducted to improve the transparency and reproducibility of this review. The databases searched included Web of Science Core Collection, Scopus, ScienceDirect, SpringerLink, ACS Publications, and Wiley Online Library. The main search period covered publications from 1988 to 2026, with priority given to peer-reviewed journal articles published in the last ten years. The following combinations of keywords were used: “plant extract corrosion inhibitor”, “green corrosion inhibitor”, “natural corrosion inhibitor”, “reinforced concrete”, “steel rebar”, “simulated concrete pore solution”, “chloride-induced corrosion”, “mortar”, “concrete”, “layered double hydroxide”, “inhibitor release”, “phenolic compounds”, “flavonoids”, “tannins”, “adsorption”, “passive film”, and “electrochemical impedance spectroscopy”. The literature screening was conducted in three sequential phases. First, duplicate records across all retrieved databases were removed. Second, title and abstract screening was performed to exclude studies deemed clearly irrelevant to the research scope. Finally, full-text articles of the remaining records were retrieved and evaluated against the predefined eligibility criteria. A total of over 260 records were initially identified through database searches. After the full screening workflow, 155 studies that satisfied all predefined eligibility criteria were ultimately included in this review.

The predefined eligibility criteria included three core inclusion requirements: (1) studies involving plant-derived, bio-based, or naturally derived organic inhibitors for steel or reinforcing steel; (2) studies reporting electrochemical, gravimetric, surface-analytical, or cementitious-material performance data; and (3) studies relevant to acidic corrosion, saline corrosion, simulated concrete pore solutions (SCPS), mortar, or concrete systems. Studies were excluded if they focused on non-plant-derived inhibitors or non-steel metal substrates, failed to report complete, usable experimental data, involved corrosion systems beyond the predefined scope of this review, were non-peer-reviewed documents such as conference abstracts, dissertations, and patents, or were review articles without original experimental data.

3. Chloride-Induced Corrosion of Steel Reinforcement in Concrete and Its Mitigation

3.1. Corrosion Mechanism of Steel Reinforcement Under Chloride Attack

As the most dominant aggressive medium in RC structures, chloride-induced corrosion leads not only to superficial damage such as concrete cracking and spalling, but also to effective cross-section loss of steel rebars and degradation of steel-concrete bond performance via the volumetric expansion effect of corrosion products, ultimately resulting in deterioration of structural load-bearing capacity [24,25]. Typical corrosion deterioration of RC structures under long-term chloride attack is shown in Figure 1.

Figure 1. The corrosion and deterioration of reinforced concrete buildings exposed to a marine environment. (**a**,**b**) Extensive concrete deterioration requiring major structural intervention; (**c**) column before concrete removal works; and (**d**) column after concrete removal works. Reprinted from Ref. [26].

Therefore, systematically elucidating the microscopic mechanism of chloride-induced steel corrosion in a concrete environment can provide useful support for formulating scientific protection strategies and extending the service life of RC structures. From a macroscopic perspective, chloride-induced steel corrosion in concrete is a multi-stage coupled process covering ion transport, passive film breakdown, electrochemical corrosion, and corrosion product expansion, as schematically illustrated in Figure 2.

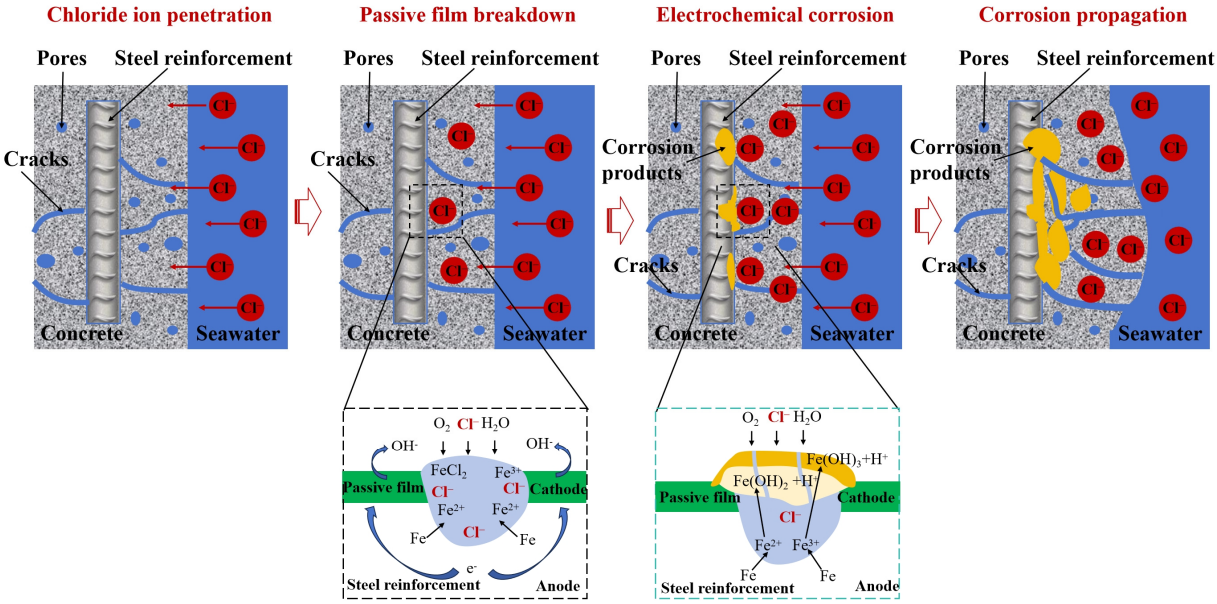

Figure 2. The whole process of chloride-induced steel corrosion in concrete.

The whole process can be divided into four sequential stages:

1. **Chloride ion penetration stage**

Chloride ions migrate through the concrete pore network via multiple mechanisms, including diffusion, capillary suction, electromigration, and pressure-driven permeation. Under water-saturated conditions, Fickian diffusion driven by a concentration gradient is the dominant transport mechanism; under wetting-drying cycling conditions, capillary action significantly accelerates the non-steady-state transport of chloride ions [4,27,28]. The transport rate is governed by concrete properties such as water-to-binder ratio, pore structure, mineral admixture type, as well as ambient temperature and humidity. Chloride ions eventually reach the steel surface through concrete capillary pores and microcracks.

2. **Passive film breakdown stage**

A dense passive film mainly composed of iron oxides/hydroxides naturally forms on the steel surface in the highly alkaline concrete environment, which inhibits active corrosion of steel. When the free chloride concentration at the steel surface reaches the critical threshold, the protective passive film begins to break down locally, exposing the underlying steel to corrosive media and initiating corrosion [29,30].

3. **Electrochemical corrosion stage**

Once the passive film fails, electrochemical corrosion reactions proceed on the steel surface in the presence of oxygen and moisture. Iron is initially oxidized to ferrous hydroxide ($Fe(OH)_2$) and subsequently converted into iron oxides, such as Fe_2O_3 and Fe_3O_4. Since the resulting corrosion products have a volume about 2–6 times larger than that of the original steel, internal tensile stresses develop in the surrounding concrete, which may eventually cause cracking and spalling [31].

4. Corrosion propagation and deterioration stage

The accumulation and expansion of corrosion products sustain the ongoing oxidation of the steel surface, while their volumetric expansion further enlarges existing concrete cracks. This establishes a detrimental feedback loop in which cracking accelerates the ingress of chloride ions and oxygen, thereby intensifying steel corrosion and promoting the progressive deterioration of RC structures [32].

At the microscale, two classical theoretical models are widely accepted to explain the passive film breakdown mechanism induced by chloride ions: the ion exchange model (IEM) and the point defect model (PDM) (Figure 3). According to the ion exchange model, pit nucleation follows three steps: adsorption of chloride ions on the passive film surface, corrosive attack via ion exchange between chloride ions and surface oxygen or oxygen vacancies, and inward migration of chloride ions through the passive film (Figure 3a) [33].

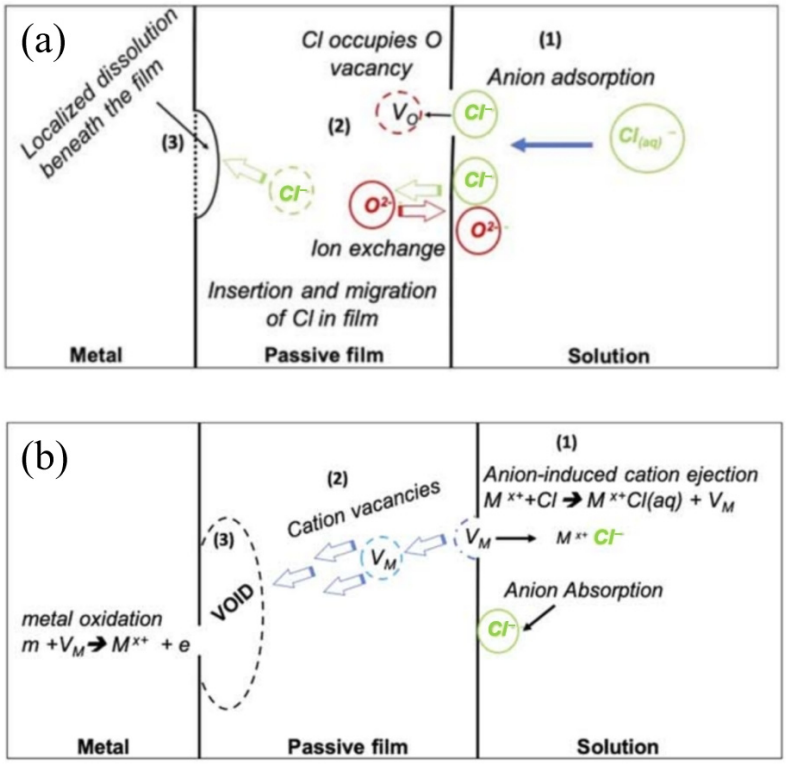

Figure 3. Schematic diagram of passive film breakdown mechanism. (**a**) IEM; and (**b**) PDM. Reprinted from Ref. [33].

The PDM proposes that chloride ions adsorbed on the passive film catalyze the formation of cation vacancies at the metal surface (Figure 3b) [33]. The process begins with surface cations forming a complex with chloride ions and gently detaching from the surface; next, the resulting cation vacancies migrate toward the metal/oxide interface; finally, these vacancies gradually accumulate locally, leading to the formation of a small void at the metal/film interface [33,34].

Therefore, chloride-induced steel corrosion is a complex dynamic process driven by the coupling of ion transport, interfacial reaction, electrochemistry, and mechanical damage. An in-depth understanding of the above process and mechanism provides the theoretical foundation for developing high-efficiency protection technologies and constitutes the core basis for scientifically evaluating the performance of various corrosion inhibition techniques.

3.2. Control Strategies for Steel Reinforcement Corrosion in Concrete

As summarized in Figure 4, three mainstream protective technologies have been developed to address chloride-induced corrosion of steel reinforcement, namely surface coatings, high-performance concrete, and corrosion inhibitors. Among these, plant-based corrosion inhibitors are emerging as a promising research direction due to their environmental friendliness, renewable feedstocks, and cost advantages.

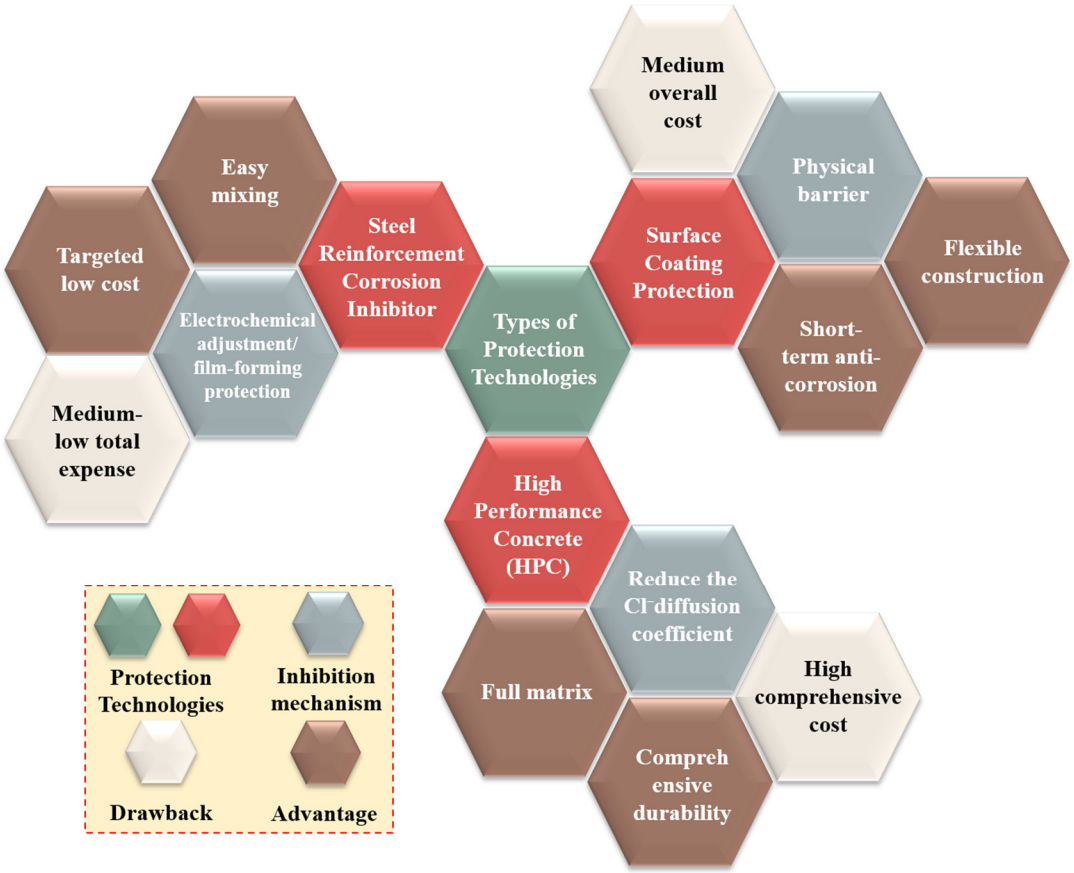

Figure 4. Control strategies for steel reinforcement corrosion in concrete.

3.2.1. Protective Surface Coating Technology

Protective surface coatings form a dense physical barrier on steel reinforcement or concrete surfaces, blocking the transport of aggressive media (chloride ions, oxygen, and moisture) to the steel-concrete interface (Figure 4). Commonly used engineering coating systems include epoxy-based, polyurethane-based, acrylic-based, and polymer-modified cementitious coatings [35–40]. This technology is widely applied in engineering practice for its direct inhibition effect on the steel surface and convenient construction process [41].

Nevertheless, coating systems still have notable limitations in long-term service [42]. First, their environmental adaptability and durability may be insufficient: under ultraviolet (UV) radiation, load impact, and high-salinity marine attack, coatings are prone to cracking and delamination, leading to premature loss of protective function [24]. Second, the final protection performance is highly dependent on construction quality; the uniformity and thickness control of on-site coating application remains a technical bottleneck for large-scale engineering promotion [43].

3.2.2. High-Performance Concrete (HPC) Technology

High-performance concrete (HPC) achieves high matrix densification and pore structure refinement through a low water-to-binder ratio, optimized mineral admixture blending

(fly ash, slag, silica fume, etc.), and superplasticizer synergism [44]. This fundamentally reduces the chloride diffusion coefficient and significantly prolongs the passive state of steel reinforcement (Figure 4). The core advantages of HPC are reflected in these aspects: high compressive strength to meet high design load requirements; markedly enhanced matrix compactness to reduce water and chloride permeation and retard steel corrosion; and stable service performance under harsh environments, endowing excellent long-term durability [45,46].

However, the engineering application of HPC is also restricted by several factors. First, it entails relatively high material costs and stringent construction requirements: improper construction procedures will directly impair the mechanical properties and durability of the material, weakening its corrosion protection effect. Second, it exhibits non-negligible shrinkage deformation and cracking risk [47,48].

3.2.3. Reinforcement Corrosion Inhibitor Technology

As shown in Figure 5, corrosion inhibitors for steel reinforcement are chemical substances admixed into fresh concrete (admixed type) or applied onto hardened concrete surfaces (migrating type) to effectively suppress or retard steel corrosion [13,17]. They are currently recognized as one of the most cost-effective and construction-friendly steel protection technologies [35]. Based on chemical components, mechanisms, and application forms, corrosion inhibitors can be classified into conventional systems and emerging intelligent systems (Figure 5).

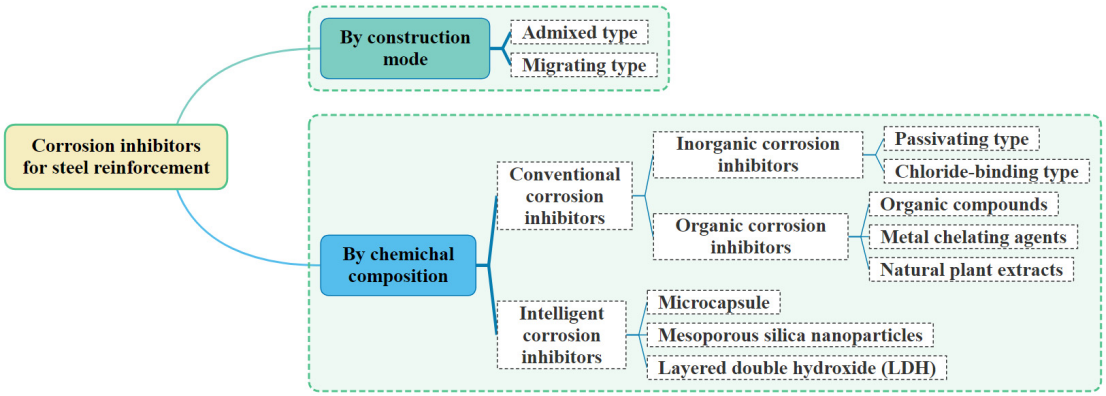

Figure 5. Classification of corrosion inhibitors for steel reinforcement.

According to chemical composition (Figure 5), conventional corrosion inhibitors are mainly divided into inorganic and organic categories [17,49]. Inorganic corrosion inhibitors function primarily by regulating the chemical environment at the steel-concrete interface and can be further subdivided into passivating type and chloride-binding type (Figure 5). Passivating inhibitors form a dense oxide film on the steel surface via interfacial reactions, isolating aggressive media from the steel substrate; typical representatives include chromates, nitrites, phosphates, molybdates, and silicates [50–55]. The typical inhibition mechanism of inorganic molybdate corrosion inhibitors is presented in Figure 6. In general, molybdates may promote the formation of $CaMoO_4$ precipitates and interact with iron oxides on the steel surface to generate protective $FeMoO_4$- and $Fe_2(MoO_4)_3$-containing films, thereby suppressing active steel corrosion [51,56]. Chloride-binding inhibitors, such as aluminates, convert free Cl^- into stable Friedel's salt or Kuzel's salt via chemical immobilization, reducing the interfacial free chloride concentration at the steel-concrete interface [57].

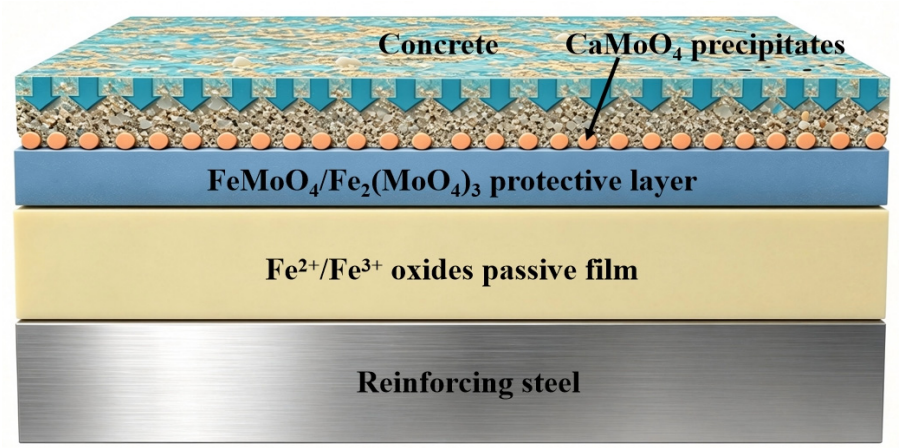

Figure 6. Schematic diagram of film formation and precipitation mechanism of molybdate on reinforcing steel surface.

The active components of organic corrosion inhibitors mainly include organic compounds, metal chelating agents, and natural plant extracts (Figure 5). Their inhibition mechanisms mainly involve organic film formation, metal ion complexation, and surface adsorption, which effectively suppress the steel corrosion process [58]. Organophosphorus inhibitors, as traditional organic systems, can form protective films via chemical reactions with the steel surface [59]; despite their favorable adsorption and anti-corrosion performance, their environmental compatibility remains controversial [60]. In addition, organic acid inhibitors represented by oxalic acid and acetic acid react with surface oxides on steel to reduce surface oxidation activity, thus achieving corrosion inhibition [61].

In particular, plant-based corrosion inhibitors have attracted widespread attention for their potential environmental advantages [15]. They form a compact protective layer at the steel interface via surface adsorption to block the penetration of aggressive media such as chloride ions; some plant-derived acid components also retard steel corrosion through excellent metal ion complexation [58,62,63]. As an important direction in developing new-generation corrosion inhibitors, plant-based systems are more comprehensively reviewed in Section 4.

In recent years, stimuli-responsive intelligent corrosion inhibitors have emerged as a prominent research focus to mitigate steel corrosion induced by the two primary degradation mechanisms: chloride ion ingress and concrete carbonation [64,65]. These inhibitors employ nano-carriers such as microcapsules, mesoporous silica nanoparticles, and layered double hydroxides (LDHs) as matrices to encapsulate active inhibiting molecules [66,67], thereby enabling Cl^--responsive controlled release or pH-responsive on-demand release via molecular gating mechanisms. The $CeMoO_x$ self-healing conversion film developed by An et al. can trigger a self-healing effect when damaged above the pitting potential, with MoO_4^{2-} within the film selectively regulating ion adsorption behavior (Figure 7) [68]. In concrete environments containing Cl^-, molybdates weaken the adsorption of Cl^- on the film surface, thereby reducing the risk of pitting corrosion (Figure 7). As corrosion progresses, multivalent redox transformations involving Ce, Mo, and Fe occur within the film, where lower-valent ions are incorporated to reduce oxygen vacancies and promote film densification, enhancing protective performance (Figure 7). Additionally, pH reduction caused by localized corrosion promotes the dissociation of molybdates into large poly-anions, which adsorb at defect sites to further enable self-repair of damage.

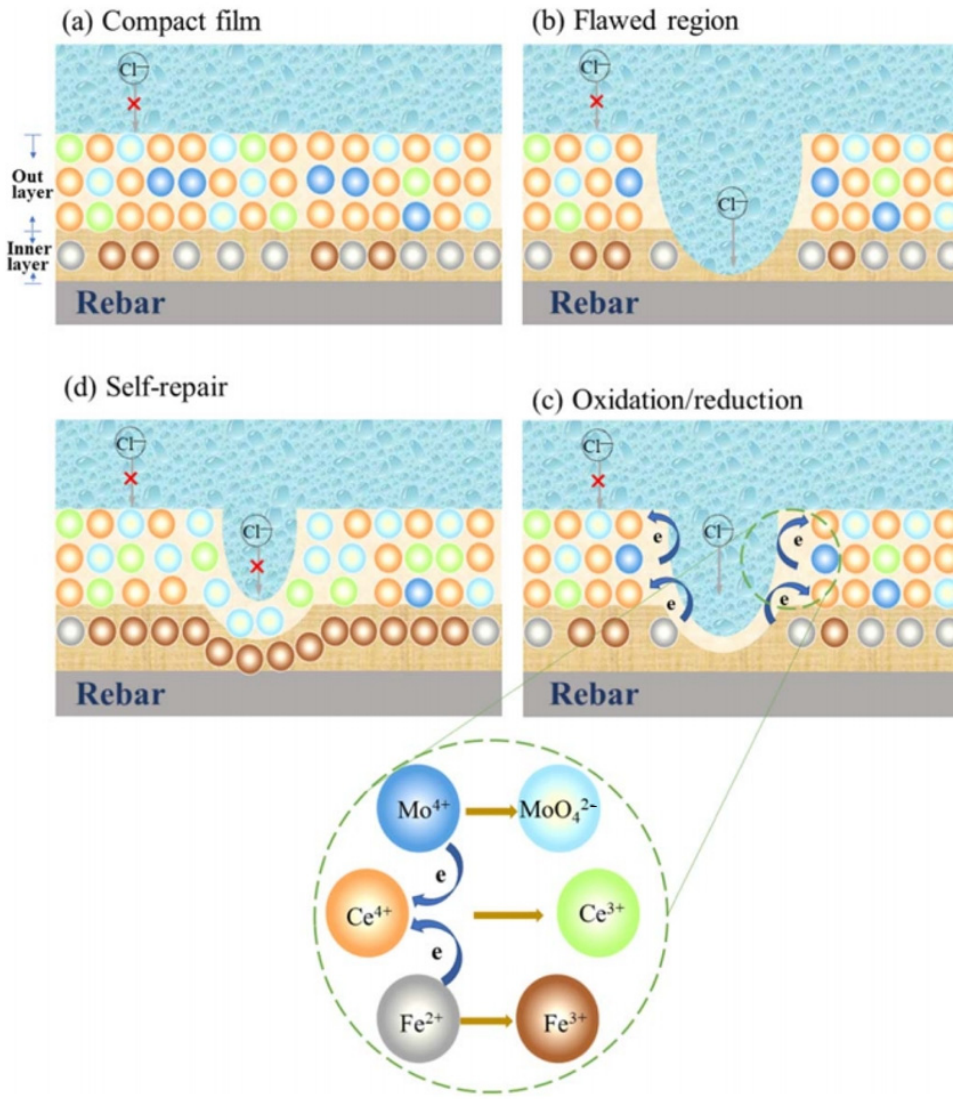

Figure 7. The self-healing and chelation synergistic protection mechanism of microcapsules. The "x" indicates effective suppression of chloride ion adsorption at the dense protective film location, thereby protecting the rebar from corrosion. Reprinted from Ref. [68].

4. Plant-Based Corrosion Inhibitors for Steel Reinforcement

Environmentally friendly (green) corrosion inhibitors mainly cover rare earth-based inorganic systems, as well as organic categories including plant-based, amino acid-based, and biopolymer inhibitors. Among them, plant-based inhibitors derived from natural biomass have become a research hotspot for new-generation reinforcement corrosion inhibitors, owing to their wide feedstock availability, low cost, low ecotoxicity, and excellent biodegradability. Representative studies, such as the green tea extract inhibitor reported by Pradipta et al. [69], have exhibited inhibition performance comparable to or even superior to conventional chemical inhibitors.

4.1. Main Types of Plant-Based Corrosion Inhibitors

Plant-based corrosion inhibitors can be systematically classified from multiple dimensions according to active component composition, mechanism, and formulation form (Figure 8).

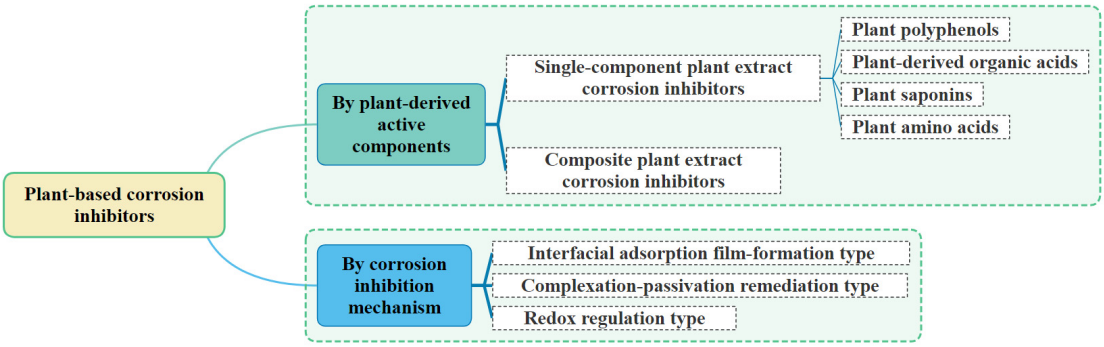

Figure 8. Schematic diagram of the classification system for plant-based corrosion inhibitors.

4.1.1. Classification by Plant-Derived Active Components

(1) **Single-component plant extract corrosion inhibitors**

Single-component inhibitors are prepared by extracting and enriching active constituents from specific plant materials, and exert corrosion inhibition via the inherent physicochemical properties of the active molecules. Current research mainly focuses on four categories of highly active plant resources: polyphenols, organic acids, saponins, and amino acid derivatives (Figure 8).

- **Plant polyphenols** are natural antioxidant substances widely distributed in tea leaves, fruits, and leaves. Their molecules are rich in phenolic hydroxyl groups and aromatic conjugated structures, which are the main contributors to corrosion inhibition activity.
- **Plant-derived organic acids**, including citric acid, oxalic acid, malic acid, and phytic acid, are characterized by strong metal-chelating ability originating from carboxyl or phosphate functional groups.
- **Plant saponins** are natural amphiphilic surfactants with good emulsifying ability and certain antioxidant properties.
- **Plant amino acids**, such as arginine and glutamic acid, exhibit good alkaline stability and biocompatibility, and contain both amino and carboxyl groups in their molecular structures.

(2) **Composite plant extract corrosion inhibitors**

Composite inhibitors are typically developed by combining multiple plant-derived active components with complementary functions to achieve synergistic improvement in corrosion inhibition performance [70]. Current composite systems mainly include two forms: inter-plant component compounding, and plant extract compounded with a small proportion of low-toxicity conventional inhibitors.

4.1.2. Classification by Corrosion Inhibition Mechanism

From the perspective of inhibition mechanism, plant-based corrosion inhibitors can be divided into three categories, corresponding to different protective pathways (Figure 8):

(1) **Physical adsorption-type plant-based inhibitors** mainly rely on the adsorption of active molecules on the metal surface to form a compact protective layer, thereby blocking the transport of corrosive species. Natural constituents in plant extracts, including polyphenols, lipids, and flavonoids, can adsorb onto the metal interface through electrostatic interactions, van der Waals forces, or hydrogen bonding. Liu et al. developed a green reinforcement corrosion inhibitor from waste *Platanus* × *acerifolia* leaves [71]. Electrochemical results indicated that the plant extract significantly reduced the corrosion rate of reinforcing steel. The inhibition effect was mainly attributed to the adsorption of polyphenol- and flavonoid-containing molecules on the steel surface,

which formed a protective organic film and blocked the diffusion of chloride ions and oxygen.

(2) **Chemical interaction-type plant-based inhibitors** inhibit the corrosion of steel through coordination, chemisorption, or deposition reactions between active constituents and the metal surface, leading to the formation of a more stable interfacial protective layer. Plant-derived organic acids, polyphenols, and flavonoids contain active functional groups such as carboxyl, hydroxyl, and carbonyl groups, which can coordinate with Fe^{2+}/Fe^{3+} ions to form metal–organic complexes. Anitha et al. [72] characterized the molecular structure of *Rosa damascene* leaf extract by ATR-FTIR, and further analyzed the valence states and chemical composition of the passive film on inhibited reinforcing steel using XPS, thereby proposing a physical model for the inhibitor-modified passive layer.

(3) **Bioactive type plant-based inhibitors** refer to green corrosion-inhibiting materials that utilize natural bioactive constituents from plant extracts to suppress corrosion. These compounds can form protective adsorption films on metal surfaces and may also exhibit antibacterial, antioxidant, and environmental adaptability, which is beneficial for mitigating microbiologically influenced corrosion and other environmental corrosion processes. Representative examples of bioactive plant-based inhibitors include neem leaf extract (*Azadirachta indica*) and clove essential oil (*Syzygium aromaticum*) [73,74].

4.2. Performance Evaluation and Mechanism Elucidation Methods for Plant-Based Corrosion Inhibitors

Plant-based corrosion inhibitors feature highly complex chemical compositions, with only specific active components contributing to corrosion inhibition. Therefore, screening and purification of active constituents, quantitative evaluation of inhibition performance, and systematic elucidation of mechanisms constitute core prerequisites for the development and engineering application of high-efficiency plant-based inhibitors (Figure 9). This section summarizes commonly used research methods from three dimensions: active component screening, performance evaluation, and multi-scale mechanism analysis.

4.2.1. Screening and Identification of Active Corrosion-Inhibiting Components

Quantum chemical calculation is a typical theoretical screening method: it evaluates the adsorption activity and inhibition potential of molecules by analyzing electronic structure parameters (frontier molecular orbital energy, energy gap, electrostatic potential distribution, etc.) and identifying reactive sites within molecules [75] (Figure 9). For instance, Hou et al. [76] compared the theoretical inhibition efficiency of B-group vitamins and vitamin C via DFT+U calculations. Such theoretical methods provide efficient guidance for targeted screening of active components.

Quantitative determination of bioactive constituents underpins the screening of core inhibitory components, establishment of structure-activity relationships, and quality control of plant-based inhibitors. Given the multicomponent nature of plant extracts, multiple analytical strategies have been developed for different detection targets (Figure 9). Spectrophotometric methods are commonly employed for rapid quantification of total active fractions. The Folin–Ciocalteu assay is typically used to determine total phenolic content, while the aluminum nitrate colorimetric method is applied to total flavonoid measurement [77]. For individual compounds, high-performance liquid chromatography (HPLC) enables accurate analysis of non-volatile constituents [78], such as polyphenols and organic acids, as reported for *Caesalpinia spinosa*, *Olea europaea* L., and *Platanus* × *acerifolia*. Gas chromatography–mass spectrometry (GC-MS) is suitable for semi-quantitative identification of volatile and lipophilic compounds through peak area normalization, as shown in the analysis of *Rosa damascena* extracts [79]. Additionally, Liquid chromatography–tandem

mass spectrometry (LC-MS/MS) further provides high sensitivity for trace polar components, enabling detailed characterization of minor bioactive constituents in complex plant matrices [80].

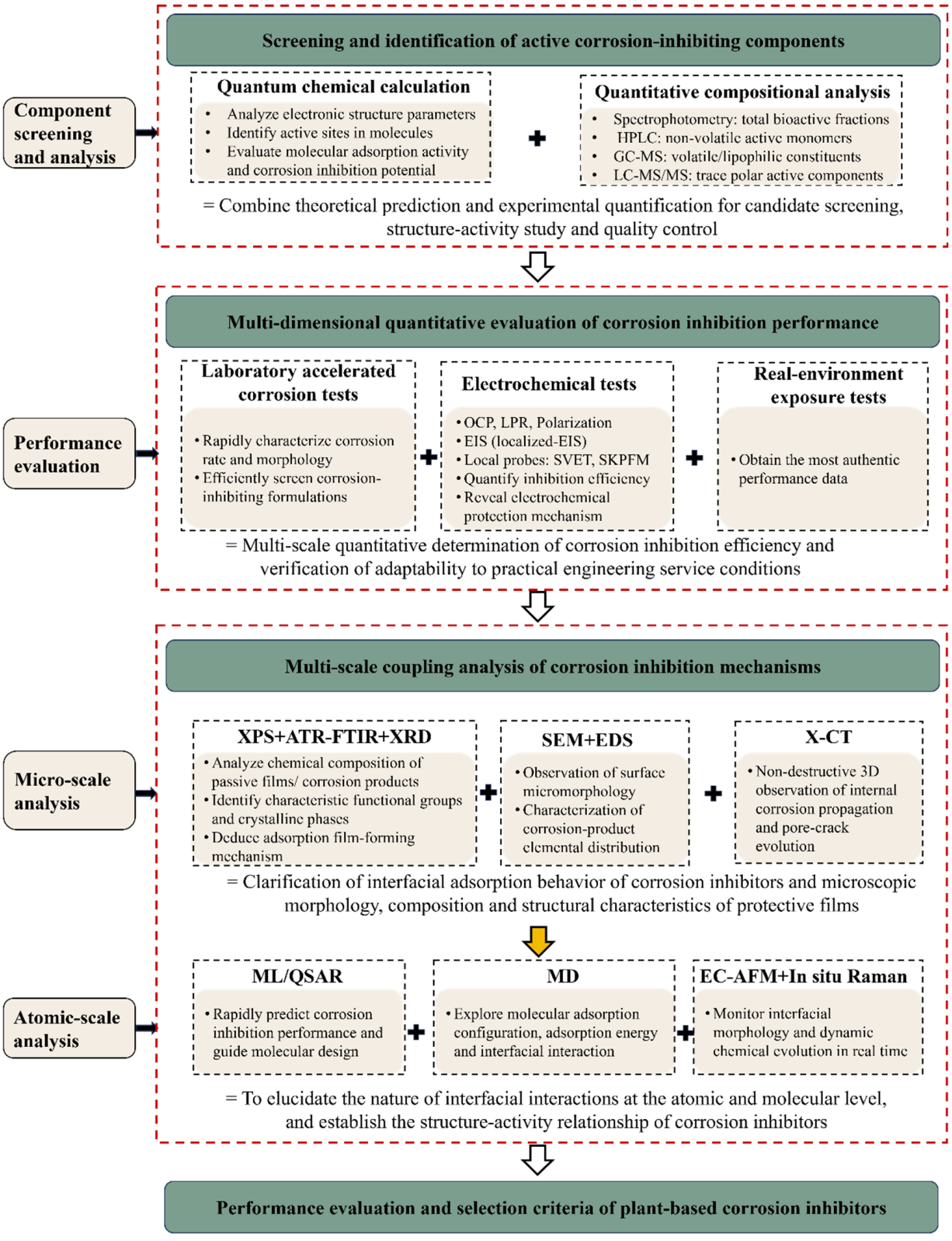

Figure 9. The flowchart for evaluating the inhibitory efficiency and exploring the inhibition mechanism of plant-based corrosion inhibitors.

4.2.2. Evaluation Methods for Corrosion Inhibition Performance

A scientific performance evaluation system is essential for verifying the protective effect of inhibitors and supporting engineering applications. Current mainstream evaluation methods can be broadly divided into three categories.

(1) **Laboratory accelerated corrosion tests**

Laboratory accelerated corrosion tests are widely used to evaluate the durability and inhibition efficiency of protective systems within a shortened testing period (Figure 9). Common methods include neutral salt spray tests in accordance with ASTM B117 [81], cyclic or modified salt fog tests according to ASTM G85 [82], immersion tests in SCPS or chloride-containing media, and macrocell corrosion tests for reinforced concrete systems according to ASTM G109 [83]. These methods simulate chloride-induced corrosion conditions typically encountered in marine, de-icing salt, and salt-lake environments by exposing specimens to aggressive media such as high-concentration chloride solutions, artificial seawater, or cyclic wet-dry conditions [84,85].

The corrosion protection performance is generally assessed by monitoring the time to corrosion initiation, corrosion product formation, mass loss, corrosion penetration depth, surface morphology, cracking of concrete cover, chloride penetration depth, and corrosion product distribution. For steel coupons, gravimetric mass-loss measurements after removal of corrosion products can provide a direct estimate of the average corrosion rate. For reinforced mortar or concrete specimens, corrosion evaluation is usually combined with half-cell potential measurements, macrocell current monitoring, crack-width observation, and post-exposure examination of the steel surface [86].

(2) **Electrochemical tests**

Electrochemical techniques are among the most widely used methods for evaluating corrosion inhibitors, enabling real-time quantification of corrosion rates and early detection of localized degradation (Figure 9). Common electrochemical methods include open-circuit potential (OCP) monitoring, half-cell potential method, linear polarization resistance (LPR), potentiodynamic polarization, and electrochemical impedance spectroscopy (EIS) [87].

OCP monitoring provides information on the thermodynamic tendency of steel toward corrosion in a given environment. In RC structures, the half-cell method, commonly conducted in accordance with ASTM C876 [88], is frequently used for on-site assessment of corrosion probability [84]. LPR can be used to estimate the polarization resistance, which is inversely related to the corrosion current density through the Stern-Geary relationship [37].

Potentiodynamic polarization measurements provide key electrochemical parameters, including corrosion potential, corrosion current density, anodic and cathodic Tafel slopes, and pitting potential [89]. These parameters are useful for identifying whether an inhibitor mainly suppresses the anodic metal dissolution reaction, the cathodic oxygen reduction reaction, or both. For plant-based inhibitors, polarization curves are commonly used to determine whether the extract behaves as an anodic, cathodic, or mixed-type inhibitor. For example, Song et al. [71] employed multiple electrochemical methods to evaluate the inhibition performance of *Platanus* leaf extract on steel reinforcement.

EIS measurements provide more detailed information on interfacial corrosion processes [90]. By applying a small-amplitude alternating perturbation over a wide frequency range, EIS can resolve the complex and overlapping physical structures of a corroding system into individual electrical components [91]. For reinforced cementitious systems, the impedance response can be fitted using equivalent circuits containing solution resistance, passive-film resistance, charge-transfer resistance, constant phase elements, and diffusion-related Warburg impedance [92,93]. Therefore, EIS can distinguish between electrolyte transport through pores, protective-film formation, charge-transfer reactions at

the steel/electrolyte interface, and diffusion-controlled processes. An increase in charge-transfer resistance or film resistance generally indicates improved corrosion protection. In addition, localized electrochemical techniques, such as localized EIS, scanning vibrating electrode technique (SVET), and scanning Kelvin probe force microscope (SKPFM), can further reveal spatially heterogeneous corrosion and early pitting behavior [94,95].

(3) **Real-environment exposure tests**

Real-environment exposure tests place specimens in actual service scenarios (marine atmosphere, industrial atmosphere, etc.) for long-term observation (Figure 9). Although time-consuming, they can provide performance data closest to real engineering conditions. China's National Materials Environmental Corrosion Platform has established multiple marine test stations covering temperate to tropical sea areas, which are widely used for long-term durability validation of concrete materials.

4.2.3. Multi-Scale Elucidation of Corrosion Inhibition Mechanisms

Clarifying inhibition mechanisms at the microscale is critical for guiding the performance optimization of plant-based inhibitors. Current research mainly relies on surface analysis, in situ and 3D visualization characterization, and theoretical simulation to reveal the interfacial behavior and protective essence of inhibitors (Figure 9).

(1) **Surface analysis techniques**

Surface analysis techniques are essential for revealing the protective mechanism of plant-based inhibitors at the steel/electrolyte interface. Scanning electron microscopy (SEM) combined with energy-dispersive spectroscopy (EDS) can directly observe surface morphology, corrosion pits, corrosion-product distribution, and elemental composition [62]. X-ray diffraction (XRD) can identify crystalline corrosion products, such as iron oxides, iron oxyhydroxides, and chloride-containing phases [86]. Fourier-transform infrared spectroscopy (FTIR) and attenuated total reflectance FTIR (ATR-FTIR) can identify organic functional groups involved in inhibitor adsorption, such as hydroxyl, carbonyl, carboxyl, amino, and aromatic groups [86].

X-ray photoelectron spectroscopy (XPS) is particularly useful for determining the chemical composition, elemental valence state, and bonding environment of interfacial protective films [96]. It can provide evidence for the formation of metal–organic complexes, adsorption layers, and stable passive films. For example, Anitha et al. [72] combined ATR-FTIR and XRD to characterize the passive film composition on steel treated with *Rosa damascene* leaf extract and proposed a corresponding protection model. These surface-sensitive methods help clarify whether the inhibition effect arises from physical adsorption, chemisorption, complexation with iron ions, passive-film stabilization, or barrier-film formation.

(2) **Three-dimensional visualization and in situ characterization**

X-ray computed tomography, including micro-CT, has been widely used to non-destructively characterize pore structure, internal cracking, corrosion-product accumulation, and transport-related damage in cementitious materials [97]. In reinforced cementitious systems, this technique can provide three-dimensional information that complements electrochemical measurements and surface characterization.

In situ characterization techniques, such as electrochemical atomic force microscopy (EC-AFM) and in situ Raman spectroscopy, enable real-time monitoring of interfacial morphological and chemical changes during the corrosion inhibition process [98,99]. EC-AFM can monitor nanoscale changes in passive-film morphology, local dissolution, and adsorption layers under electrochemical control, whereas Raman spectroscopy can identify corrosion products and iron oxide/hydroxide phases formed on the steel surface. Therefore, their

combined use is valuable for distinguishing physical adsorption, chemisorption, passive-film stabilization, and localized breakdown processes in alkaline chloride-containing pore solutions [100].

(3) **Theoretical calculations and simulations**

Molecular dynamics (MD) simulations can further investigate the adsorption configuration, adsorption energy, surface coverage, and interaction between inhibitor molecules and metal surfaces. These methods can reveal whether inhibitor molecules preferentially adopt parallel or tilted adsorption orientations and whether they are capable of forming compact protective films on iron or steel surfaces. Diamanti [75] employed MD simulations to investigate the interaction between organic corrosion inhibitors and steel reinforcement surfaces, and established a kinetic model for inhibitor adsorption and film formation. For plant extracts containing multiple active compounds, simulations can help identify the dominant corrosion-inhibiting constituents as well as possible synergistic interactions among them [75,101]. In addition, with the rapid development of artificial intelligence, machine learning-based quantitative structure-activity relationship (QSAR) models have been increasingly applied to enable rapid performance prediction of novel inhibitors, thereby providing guidance for molecular design [102,103].

Overall, the integration of multi-scale experimental characterization with computational analysis is necessary for establishing reliable structure–activity relationships and guiding the rational design of next-generation plant-based corrosion inhibitors.

4.3. Research Progress of Typical Plant-Based Corrosion Inhibitors

4.3.1. Reported Plant-Based Corrosion Inhibitors for Steel in Different Test Environments

The reported plant-based corrosion inhibitors for steel in different test environments are summarized in Table 1. In acidic HCl or H_2SO_4 solutions, steel corrosion is generally dominated by active dissolution and hydrogen evolution, and plant extracts mainly inhibit corrosion through adsorption on actively dissolving steel surfaces [104–109]. By contrast, in alkaline concrete pore solutions, reinforcing steel is initially protected by a passive film, and chloride-induced corrosion involves passive-film destabilization, localized breakdown, and pitting [72,110–116]. Therefore, inhibition efficiencies obtained in acidic media, such as those reported for grape-seed and Ginkgo leaf extracts in HCl [104,105], should not be directly extrapolated to reinforced concrete under chloride attack. Such studies are useful for identifying potentially active molecular structures, such as phenolic hydroxyl, carbonyl, and heteroatom-containing groups; however, validation in SCPS, mortar, or concrete specimens is necessary before their applicability to reinforced concrete can be established.

(1) **Extraction protocols and purity characterization of plant-based corrosion inhibitors**

As summarized in Table 1, current studies on plant-based corrosion inhibitors exhibit substantial non-standardization in extraction protocols and purity characterization, which limits the comparability of reported results and hinders a clear understanding of the relationship between extract composition and corrosion-inhibition performance.

Table 1. Reported plant-based corrosion inhibitors for steel in different test environments, including acidic media, neutral saline solutions, SCPS, and cementitious systems.

System Category	Plant Extract	Source	Extraction Method	Active Components	Concentration (wt.%)	Test System	Mechanism	Inhibition Efficiency (%)	Ref.
Acidic solution system	Grape seed	Purchased from Ebnemasouye Co.	/	Flavonoids such as catechin, epicatechin, and some phenolic acids	0.01–0.03	1 M HCl	Chemically adsorbs onto steel substrates and forms stable complexes with Fe^{3+}	92.0	[104]
	Grape seed	Purchased from Chemiloids, India	/	Proanthocyanidins	0.024	1 M sulfamic acid	Physical adsorption	65.0	[106]
	Caesalpinia spinosa	Purchased from a local producer, Ecuador	Soxhlet/Maceration (ethanol-water)	Gallic acid adsorbate	0.02–0.10	0.1 M HNO_3	Physical adsorption on the mild steel surface	85.3–97.4	[107]
	Corn	Purchased from Sigma-Aldrich	/	Corn peptone	0.005–0.050	1 M HCl	Both physisorption and chemisorption phenomena	70.3–95.1	[108]
	Platanus × *acerifolia* leaf	Collected from University of Science and Technology Beijing, China	Heated solvent extraction and vacuum freeze-drying	Flavonoids, flavonols, chalcones, and phenolic carboxylic acids	0.005–0.040	1 M HCl	Synergistic combination of physical and chemical adsorption mechanisms	66.6–93.1	[109]
	Ginkgo biloba	Collected from Southwest Forestry University, China	Ethanol reflux extraction, degreasing, and vacuum drying	Flavonoids, ginkgolides, and amino acids	0.0005–0.0100	1.0 M HCl and 0.5 M H_2SO_4	Adsorb on metal surface	80.0–94.8	[105]
Simulated solution system	*Ginkgo biloba* fruit	Purchased from Sigma-Aldrich	Water maceration and aqueous reflux extraction	Ginkgolides and bilobalide	0.005–0.015	SCPS, containing 0.3 M KOH, 0.1 M NaOH and 1% NaCl, saturated with $Ca(OH)_2$	Reacts with ferric ions to generate a dense protective film	67.3–89.0	[110]
	Sapota leaf	/	Soxhlet water extraction and water-bath evaporation	Electron-rich elements	0.05–0.20	3 M NaOH	Adsorb on both anodic and cathodic areas	66.8–88.0	[111]

Table 1. *Cont.*

System Category	Plant Extract	Source	Extraction Method	Active Components	Concentration (wt.%)	Test System	Mechanism	Inhibition Efficiency (%)	Ref.
Simulated solution system	Maize gluten meal	Purchased from local biological products	Solvent extraction, alkali dissolution-acid precipitation and centrifugation	Polar groups including N and O elements in amide groups	0.025–0.200	SCPS, containing 0.6 M KOH, 0.2 M NaOH and 3% NaCl, saturated with $Ca(OH)_2$	Adsorb onto active sites of rebar	62.7–88.1	[112]
	Tobacco leaf	/	Hot water reflux extraction and filtration	Nicotine	0.4–1.6	Aerated simulated saline solution containing 3.5% NaCl	Physical adsorption mechanism	22.1–55.6	[113]
	Platanus × *acerifolia* leaf	Collected from Nanjing, China	Alkaline-ultrasonic extraction and evaporation	Flavonoids and their derivatives	0.5–1.5	SCPS, containing 0.3 M KOH and 0.1 M NaOH, saturated with $Ca(OH)_2$, with 0.6% NaCl added daily for 10 days	Protective carbon-containing organic film via chelation and surface physical adsorption	69.4–99.9	[114]
	/	Purchased from Sigma-Aldrich, Seoul, Korea	/	L-Arginine	2.0	SCPS, containing 0.3 M KOH, 0.1 M NaOH, and 2.98%/4.97% NaCl, saturated with $Ca(OH)_2$	Adsorbs onto the rebar by forming a Zwitterion-Fe complex	/	[115]
	Olea europaea L.	Collected from arid zones of Dammam, Saudi Arabia	Shade drying, Soxhlet extraction, and rotary evaporation	Oleuropein, Verbacoside, active molecules bearing N/O heteroatoms and π-electrons	/	0.1 M NaOH and 2.87% NaCl with pH around 13	Adsorbs to form a protective film on steel and inhibits corrosion via phenolic antioxidants	91.9	[116]

Table 1. *Cont.*

System Category	Plant Extract	Source	Extraction Method	Active Components	Concentration (wt.%)	Test System	Mechanism	Inhibition Efficiency (%)	Ref.
Simulated solution system	*Rosa damascene*	Collected from Ooty, India	0.5 M H_2SO_4 reflux extraction and room-temperature drying (RDAE); Ethanol reflux extraction and room-temperature drying (RDEE)	Aromatic and heterocyclic compounds including 4-hydroxychalcone, esculetin (RDAE); Esters, terpenoids and saccharides including di-n-octylphthalate, botulin (RDEE)	2–12 (v/v %)	SCPS, containing 0.5 M $Ca(OH)_2$, 0.5 M KOH, 0.1 M NaOH and 2.92% NaCl	Adsorb on the steel surface via O/N/S-bearing aromatic phytoconstituents, form a protective barrier to block aggressive ions and hinder electron transfer	50.9–81.9	[72]
Mortar/cement-based system	Green tea	/	Ultrasonic hot-water extraction and drying	Epigallocatechin gallate, epicatechin gallate, and catechin (epicatechin)	2.0–3.0	Mortar containing 3.5% NaCl	Protective layer on rebar surface	75.0–80.0	[69]
	/	Purchased from E-Merck	Methanol dissolution (stock preparation)	Gallic acid	0.0625–0.2500	Mortar containing 3.5% NaCl	Protective film of FeO−Ca^{2+}-GA anion	97.9	[23]
	Maize gluten meal	/	/	Polar groups including N and O elements in amide groups	1.00	Mortar containing 3% NaCl	Adsorbs on the steel surface at the early stage of cement hydration	92.7–97.9	[117]
	Elaeis guineensis leaf	Purchased from a farm in Johor, southern Malaysia	Ethanol maceration, $AgNO_3$ reaction, and centrifugation	Tannins, alkaloids, coumarins, flavonoids, carbohydrates, etc.	5.00	Concrete slab with natural seawater	EG/AgNPs inhibit concrete corrosion by generating dense crystalline C-S-H gels via pozzolanic reaction to block capillary pores and act as a barrier against chloride ion diffusion	94.7	[118]

Note 1: All inhibitor concentrations are presented in weight percentage (wt.%), except for the Rosa damascena leaf extracts (RDAE and RDEE), which are expressed in volume percentage (v/v%). Note 2: The symbol "/" in the table indicates that the corresponding parameter was not reported in the original literature.

First, extraction and post-treatment procedures vary considerably among different studies. A variety of extraction methods have been employed, including reflux extraction [72,105,110,113], soxhlet extraction [107,111,116], ultrasonic-assisted extraction [69,114], heated solvent extraction [109], and maceration [107,118]. The extraction solvents also vary widely, ranging from deionized water, ethanol, and methanol to dilute sulfuric acid. In addition, post-extraction treatments such as concentration, drying, and purification are not standardized. For example, some extracts are dried at room temperature, whereas others are subjected to vacuum drying, freeze-drying, or rotary evaporation. Such variations in extraction and post-treatment conditions can significantly affect the composition and relative content of active constituents in the final extract, thereby contributing to the discrepancies in reported inhibition performance.

Second, the purity and chemical composition of plant-based inhibitors are insufficiently characterized in most studies [119]. The majority of reported inhibitors are crude extracts used directly without further purification, and only a limited number of studies provide quantitative information on their dominant active components. For example, the main functional constituents have been reported for *Caesalpinia spinosa* [107], *Olea europaea* L. [116], and *Platanus* × *acerifolia* [114]. However, such analyses remain uncommon, and standardized purity evaluation criteria are still lacking. This deficiency makes it difficult to correlate inhibitor performance with the actual concentration of active species and restricts the establishment of reliable structure–activity relationships.

(2) **Environmental compatibility and toxicity of plant-based corrosion inhibitors**

The environmental and toxicological profiles of plant-based corrosion inhibitors depend not only on the source material, but also on extraction processes, solvent selection, dosage, residual components, and possible environmental release during application [120,121].

From a life-cycle perspective, their environmental compatibility should not be inferred solely from renewability. Preparation of plant extracts generally involves biomass collection, drying, grinding, solvent extraction, concentration, and purification, all of which require energy and material inputs. Solvent extraction is still the most common route, with methanol, ethanol, ether, and acetone widely used to isolate active phytochemicals. However, these solvents may introduce toxicity concerns and additional energy demands during recovery, which can offset the environmental advantages of the final extract. Moreover, plant extracts often require relatively high dosages (2000–4000 ppm) to achieve only moderate inhibition efficiencies (43–75%) [120]. In reinforced concrete applications, such dosages may translate into substantial cumulative environmental loads that have received limited quantitative attention to date [120].

Moreover, the assumption that plant-derived substances are inherently non-toxic is not always justified. Many plant extracts contain secondary metabolites, such as alkaloids, saponins, tannins, and polyphenols, whose biological effects may vary with concentration and composition. Crude extracts may also contain residual solvents or unidentified minor constituents that influence their overall toxicological behavior. For corrosion protection in reinforced concrete, attention should be given to the possible leaching of organic components, their interaction with the cementitious environment, and the long-term environmental fate of released substances or degradation products. However, systematic toxicity and ecotoxicity assessments of plant-based corrosion inhibitors remain limited in the literature [120].

Environmental claims for plant-based inhibitors are often not supported by standardized evaluation criteria. Frameworks such as OSPAR and REACH assess environmental acceptability based on parameters including toxicity, biodegradability, bioaccumulation potential, and environmental persistence [120]. Most reported studies on plant-based corro-

sion inhibitors lack data corresponding to these criteria, making claims of environmental benignity difficult to verify.

4.3.2. Inhibition Mechanism of Typical Plant-Based Green Corrosion Inhibitors

(1) **Plant polyphenol-based corrosion inhibitors**

Plant extracts obtained from Ginkgo leaves, grape seeds, *Platanus* × *acerifolia* leaves, and other plant tissues are usually rich in phenolic compounds, flavonoids, tannins, and related oxygen-containing molecules. These compounds contain phenolic hydroxyl, carbonyl, and ether groups, which may participate in adsorption on steel surfaces through electron donation, hydrogen bonding, and complexation with Fe species. Such interactions are frequently invoked to explain the inhibition behavior of plant-derived extracts in acidic or chloride-containing media [122,123].

Green tea-derived polyphenols, including catechins such as epigallocatechin gallate and related phenolic antioxidants, are among the most investigated plant polyphenol systems for corrosion protection. Catechin has been shown to inhibit corrosion and promote the conversion of corrosion products on substrates [124], while green tea antioxidants have been validated for corrosion protection of steel reinforcing bars embedded in mortar [69,123]. Based on electrochemical tests and XPS evidence, Pradipta et al. [123] suggested that natural organic antioxidants in green tea can form a protective layer on embedded steel bars in mortar, thereby reducing corrosion activity under chloride ion exposure conditions.

The antioxidant nature of plant polyphenols may also contribute to corrosion inhibition. For example, gallic acid has been reported as an effective corrosion inhibitor for steel rebars in mortar, and its inhibition behavior has been studied using EIS, polarization tests, and Raman analysis of corrosion products [23]. The corresponding mechanism involved in developing a protective film of calcium gallate on rebar surfaces is shown in Figure 10.

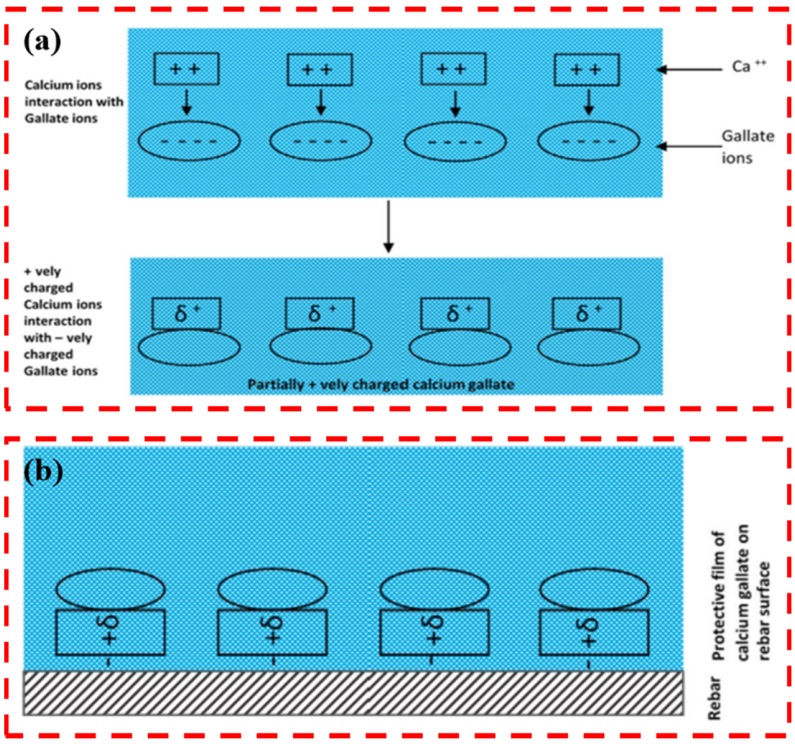

Figure 10. Mechanism involved in developing a protective film on rebar surfaces for gallic acid [23]. Reprinted from Ref. [23]. under the Creative Commons Attribution-NonCommercial-NoDerivatives 4.0 International License. (**a**) Gallic acid in concrete pore solution; and (**b**) positively charged calcium gallate electrostatically attracted towards -vely charged rebar surface.

Resveratrol-derived inhibitors have also been investigated as polyphenol-inspired green corrosion inhibitors. For chemically modified resveratrol applied to Q235 steel, UV spectroscopic analysis and DFT calculations further suggest that phenolic hydroxyl groups and π-electron-rich structures may participate in adsorption on active steel sites through electrostatic interaction and possible Fe-O coordination [125]. As another representative flavonoid-rich system, the *Ginkgo biloba* extract (EGb) has recently been evaluated as a corrosion inhibitor for carbon steel reinforcement in chloride-polluted simulated concrete pore solution [110]. Molecular dynamics simulation results demonstrate the competitive adsorption between EGb active molecules and corrosive chloride ions at the steel-solution interface. Surface characterization techniques, including SEM, AFM, optical profilometry, and XPS, support the inhibitory action of active components in GBFE. DFT and MD calculations further validate the experimental findings by elucidating the electronic properties of the active compounds.

As a typical polyphenol-rich green corrosion inhibitor, olive leaf extract acts mainly through its active phenolic components, hydroxytyrosol (HTR) and tyrosol (TRS). Lgaz et al. [126] elucidated their inhibition mechanism on Fe(110) surfaces via self-consistent-charge density-functional tight-binding (SCC-DFTB) simulations, molecular dynamics (MD) simulations, and quantum chemical calculations. As shown in Figure 11a–c, HTR adsorbs parallel to the iron surface via one Fe-O bond (2.118 Å) and two Fe-C bonds (2.238–2.3 Å), exhibiting a stronger interaction energy (−1.874 eV) than perpendicularly adsorbed TRS (−1.598 eV). Their synergistic adsorption further elevates the total interaction energy to −1.976 eV, confirming that the extra hydroxyl group in HTR strengthens interfacial bonding. PDOS analysis (Figure 11d) verifies orbital hybridization between molecular s/p orbitals and Fe 3d orbitals, revealing the chemisorption nature. HTR, with a higher HOMO level and positive electron transfer fraction (ΔN = 0.158), favors electron donation to the iron surface.

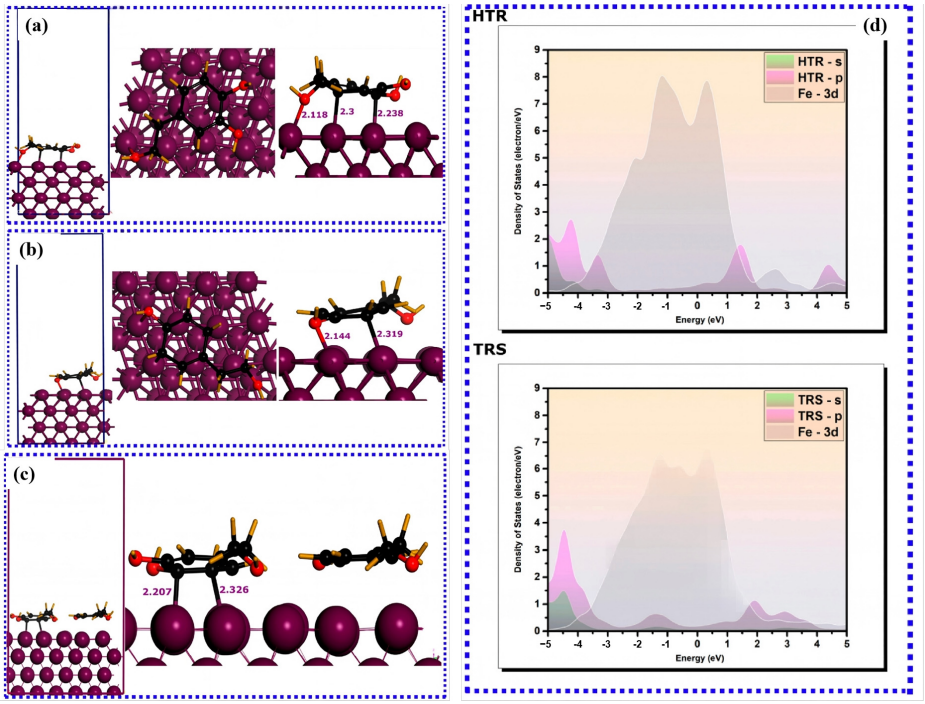

Figure 11. SCC-DFTB-optimized adsorption configurations and projected density of states (PDOS) of hydroxytyrosol (HTR), tyrosol (TRS), and their synergistic system on the Fe(110) surface. (**a**) HTR adsorption; (**b**) TRS adsorption; (**c**) HTR/TRS co-adsorption; and (**d**) PDOS spectra of adsorbed HTR and TRS systems. Reprinted from Ref. [123].

(2) **Plant organic acid-based corrosion inhibitors**

Plant-derived carboxylic acids and phosphate derivatives, mainly including citric acid, oxalic acid, malic acid, and phytic acid, are naturally occurring compounds widely found in citrus fruits, grains, and forestry by-products. These molecules contain abundant carboxylate or phosphate groups and therefore possess strong potential for metal-ion complexation. In the highly alkaline concrete pore solution, they are expected to exist predominantly in deprotonated anionic forms and may interact with Fe^{2+}/Fe^{3+} species released from defective passive films. Such interactions are commonly proposed to contribute to iron–organic complex formation, passive-film modification, and reduced penetration of aggressive species [64].

As a typical hexaphosphoric organic acid, phytic acid (PA) has attracted particular attention in RC corrosion protection due to its six phosphate functional groups and strong chelating ability [127,128]. In chloride-contaminated reinforced mortars, PA can deposit on the steel passive film and form insoluble PA–Ca and PA–Fe(III) complex layers [63]. This process extends the pitting induction period and increases the pitting potential of reinforcing steel, as confirmed by electrochemical, XPS, and FTIR analyses [63]. Citrate presents a typical concentration-dependent dual effect on steel corrosion in alkaline concrete pore solutions. At low concentrations, citrate ions adsorb on the steel surface and effectively inhibit corrosion. However, excessive citrate promotes steel dissolution due to the strong complexation between citrate and Fe^{2+}, which forms stable Fe(II)-citrate complexes and restrains the oxidation of Fe^{2+} into Fe^{3+} (Figure 12a) [129]. The addition of zinc acetate can weaken the coordination affinity of Fe^{2+} toward citrate via pre-adsorbed zinc sites on the steel surface, achieving a synergistic anti-corrosion effect (Figure 12b). These conclusions are verified by potentiodynamic polarization, half-cell potential, and FTIR spectroscopic tests [129]. Oxalic acid, a dicarboxylic acid, follows a similar chelation mechanism; it reacts with surface oxides of steel to reduce electrochemical activity and suppress localized corrosion triggered by chloride ions [130].

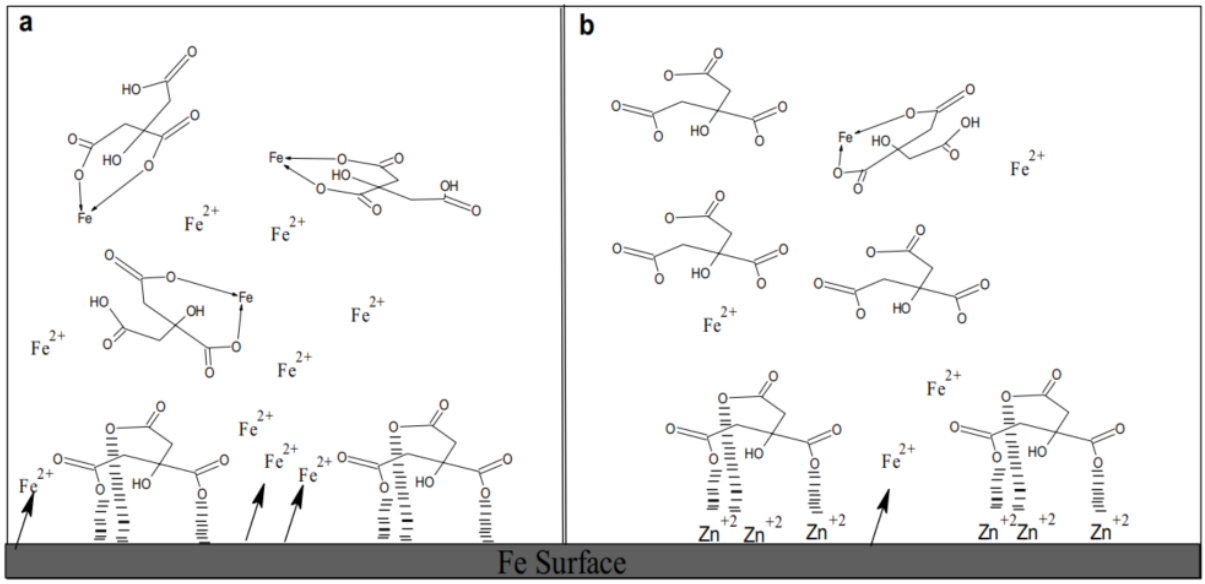

Figure 12. Corrosion inhibition mechanism of citrate for steel reinforcement. (**a**) In the absence of zinc acetate; and (**b**) in the presence of zinc acetate. Reprinted from Ref. [126].

(3) **Plant saponin-based corrosion inhibitors**

Plant saponins are natural surface-active compounds mainly extracted from *Gleditsia sinensis*, soapberry, and other plants, featuring remarkable emulsifying properties and cer-

tain antioxidant capacity [131]. Owing to their amphiphilic molecular structures, saponins are expected to adsorb at the steel-solution interface, with polar groups interacting with the steel surface or aqueous phase and hydrophobic moieties possibly extending outward. Such interfacial arrangement may increase the hydrophobicity of the steel surface and reduce the access of water, dissolved oxygen, and chloride ions to active corrosion sites.

Studies on saponin-rich *Gleditsia sinensic* extract (GSE) suggest that its corrosion inhibition is mainly associated with interfacial adsorption and protective-film formation. For example, GSE exhibited high inhibition efficiency for N80 steel in 1 M HCl, and its adsorption followed the Langmuir isotherm, with surface analyses confirming the formation of an adsorbed protective layer [132]. However, such adsorption-driven inhibition, especially when dominated by physical or weak interfacial interactions, may be less stable in highly alkaline concrete pore solutions than the coordination- or chelation-based films formed by polyphenols and organic acids. Therefore, the long-term durability of saponin-derived protective layers in reinforced concrete environments still requires further investigation.

(4) **Plant amino acid-based corrosion inhibitors**

Plant-derived amino acids, represented by glutamic acid, L-tryptophan, and methionine-containing derivatives, have attracted increasing interest as corrosion inhibitors due to their alkaline compatibility, metal-complexing ability, and excellent biocompatibility [115,133]. These molecules contain amino and carboxyl groups, and their nitrogen and oxygen atoms can donate lone-pair electrons to surface iron species, Fe^{2+}/Fe^{3+} centers, or iron oxide/hydroxide sites, thereby promoting coordination-assisted adsorption on steel surfaces [115].

Recent studies have further confirmed the potential of amino-acid-related bio-based inhibitors for steel corrosion protection in simulated concrete pore solutions [115,134,135]. Jiang et al. [134] synthesized a ferulic acid- and methionine-modified chitosan inhibitor, CTS-FA-Met, for low-carbon steel in simulated concrete pore solution. Weight-loss and electrochemical tests confirmed its high inhibition efficiency, reaching a maximum value of 96.89%, while Fe^{2+} complexation experiments and theoretical calculations revealed its strong ability to regulate dissolved iron species. Surface characterization further verified the formation of a protective interfacial film. The inhibition mechanism was therefore attributed to the combined effects of Fe^{2+} complexation and coordination-assisted adsorption, involving -NH_2, -OH, O-, and S-containing groups. More recently, Zhang et al. [135] evaluated glutamic acid in carbonated simulated concrete pore solution using OCP, EIS, PDP, adsorption thermodynamics, FTIR, 3D surface profiling, SEM-EDS, XPS, and molecular dynamics simulations. The electrochemical results showed that 1 g/L glutamic acid achieved inhibition efficiencies of 94.3% and 86.5% after 24 h and 48 h, respectively. FTIR and XPS identified the involvement of amino and carboxyl groups in surface interactions, SEM-EDS and 3D morphology confirmed the improved surface protection, and molecular dynamics simulations further supported the stable adsorption of glutamic acid on iron oxide/hydroxide surfaces.

(5) **Composite plant extract corrosion inhibitors**

Single-component plant extracts generally suffer from limitations such as a single-action mechanism, insufficient alkaline stability, and limited long-term efficiency. To address these drawbacks, composite inhibitors are developed by combining multiple active constituents with complementary mechanisms, so as to achieve synergistically enhanced corrosion inhibition performance. Liu et al. [11] experimentally demonstrated the synergistic corrosion inhibition of a phytic acid–phosphate composite on reinforcing steel in chloride-contaminated alkaline media, as evidenced by EIS, PDP, SEM/EDS mapping, and high-resolution XPS analysis. Sattari et al. [136] coupled Lavandula angustifolia (LA)

extract—rich in phenolic constituents such as ferulic acid, rosmarinic acid, and apigenin—with Zn^{2+} cations to construct an organic–inorganic hybrid inhibitor (Figure 13a). As illustrated in Figure 13b, the resulting LA-Zn^{2+} complexes operate through a dual-site mechanism: insoluble LA-Zn^{2+} chelates precipitate onto anodic regions via physisorption and chemisorption, while liberated Zn^{2+} reacts with cathodically generated OH^- to form a protective $Zn(OH)_2$ layer, yielding a synergistic inhibition efficiency of 92.8% at the optimal 400:400 ppm ratio—far exceeding that of either LA alone (46.7%) or Zn^{2+} alone (74.4%).

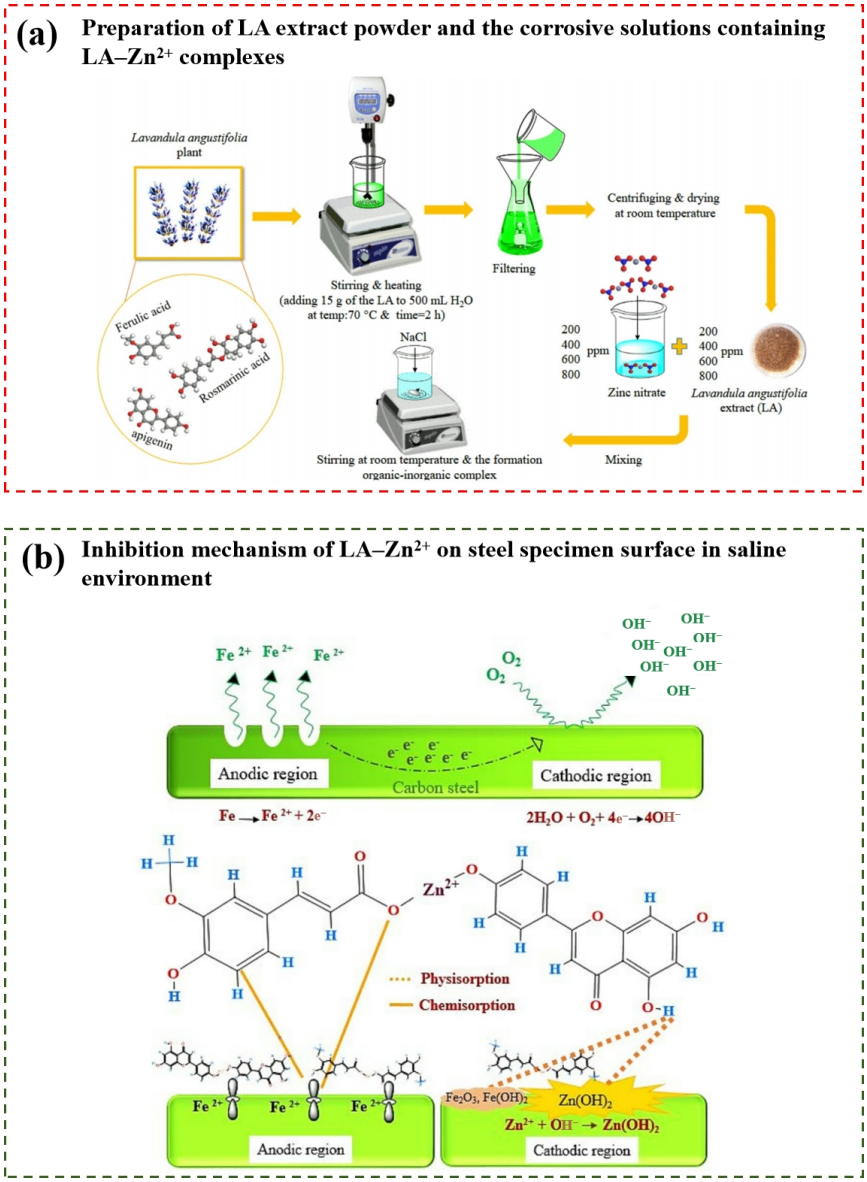

Figure 13. The synergistic inhibition mechanism of LA and Zn^{2+} systems for steel corrosion. Reprinted from Ref. [133].

In another study, Mussey et al. [137] investigated the synergistic inhibition of calcined clay pozzolan and *Acacia* leaf extract in concrete. Potentiodynamic polarization, supported by XRD and FTIR, revealed that the combination of 20% calcined clay pozzolan cement and 2% extract produced the best performance, with inhibition efficiencies of 97.1% in 3% NaCl and 95.4% in 5% NaCl. These findings highlight the potential of combining natural inhibitors with supplementary cementitious materials to improve steel corrosion resistance in chloride-contaminated concrete.

4.3.3. Compatibility and Durability of Plant-Based Inhibitors with Cement

Although many plant-based inhibitors exhibit high inhibition efficiencies in simulated pore solutions or chloride-containing mortars/concretes, such laboratory results should not be directly interpreted as evidence of engineering applicability. In RC, long-term corrosion protection depends not only on the intrinsic adsorption ability of inhibitor molecules, but also on their compatibility with cement hydration, transport through the concrete pore network, retention near the steel/concrete interface, stability under wet-dry and temperature cycles, and ability to raise the chloride threshold for corrosion initiation [138,139].

Plant extracts usually contain polyphenols, flavonoids, tannins, sugars, organic acids, and other oxygen-containing compounds, which may interact with cement particles, Ca^{2+} ions, and hydration products. Such interactions can alter hydration kinetics, setting time, heat evolution, pore structure, and early-age strength. Previous studies on organic admixtures have shown that compounds such as sucrose, tartaric acid, and lignosulfonates can significantly retard cement hydration, indicating that similar effects should be carefully considered for plant-derived inhibitors [140–142]. Therefore, their influence on setting time, hydration heat, compressive strength, phase assemblage and microstructure should be evaluated before practical use.

The long-term availability of active inhibitor species in concrete is also a key durability issue. Although admixing can initially distribute the inhibitor throughout the cementitious matrix, the effective concentration near the steel/concrete interface may decrease over time due to adsorption on C-S-H [143–145], AFm phases or calcium-rich hydration products, complexation with Ca^{2+} or Fe ions [146,147], degradation under highly alkaline pore-solution conditions, and leaching during moisture transport or wet-dry cycling [148]. Consequently, high inhibition efficiency measured in SCPS cannot be directly translated into long-term protection in concrete.

For engineering assessment, plant-based inhibitors should therefore be examined in terms of pore-solution stability, dosage retention, leaching resistance, chloride threshold improvement, and electrochemical performance under cyclic chloride exposure. Experience from conventional admixed inhibitors, such as calcium nitrite, also shows that corrosion protection in concrete is strongly dependent on inhibitor dosage, inhibitor-to-chloride ratio, and exposure conditions [146,147,149]. Thus, plant-based inhibitors should be regarded as promising but still insufficiently validated alternatives, requiring systematic concrete-based and long-term exposure studies before field application.

5. Conceptual Design and Future Perspective of a Multi-Functional EGb-LDH Inhibitor

This section takes EGb as the representative plant-derived active component and LDHs as the functional carrier, and systematically elaborates the design concept, technical characteristics, and research value of the EGb-LDH multi-functional composite system. It should be noted that this system is a theoretical design integrating two independently reported functional components (EGb as an inhibitor and LDH as a carrier), and relevant experimental verification has not been carried out in this review. Despite being at the conceptual stage, this design is built on the well-documented functional properties of both EGb and LDHs, with strong research feasibility. Follow-up experimental studies on its controllable preparation, chloride-responsive release characteristics, and cement compatibility are expected to further verify its engineering application value. This section elaborates its design framework to provide a reference for the development of intelligent green corrosion inhibitor systems.

5.1. EGb: A Representative Plant-Derived Corrosion Inhibitor

EGb, a natural active substance extracted from *Ginkgo biloba* leaves, has been widely used in pharmaceutical and healthcare fields, and also shows prominent application potential in corrosion protection. Recent studies have confirmed that EGb can achieve a corrosion inhibition efficiency of over 90% for carbon steel in harsh corrosive environments [105,150].

As depicted in Figure 14, the active components of *Ginkgo biloba* leaf extract are mainly composed of flavonoid and biflavonoid polyphenols represented by isorhamnetin and sciadopitysin, together with auxiliary active fractions such as organic acids and vitamin derivatives including 6-hydroxykynurenic acid and 4-O-methylpyridoxine (Figure 14), which endow EGb with strong interfacial adsorption capacity and the ability to form a stable protective film on steel surfaces [150]. In terms of resource attributes, China has extremely abundant ginkgo leaf resources. Utilizing active components extracted from fallen ginkgo leaves as green corrosion inhibitors not only reduces production costs, but also promotes the high-value recycling of biomass resources.

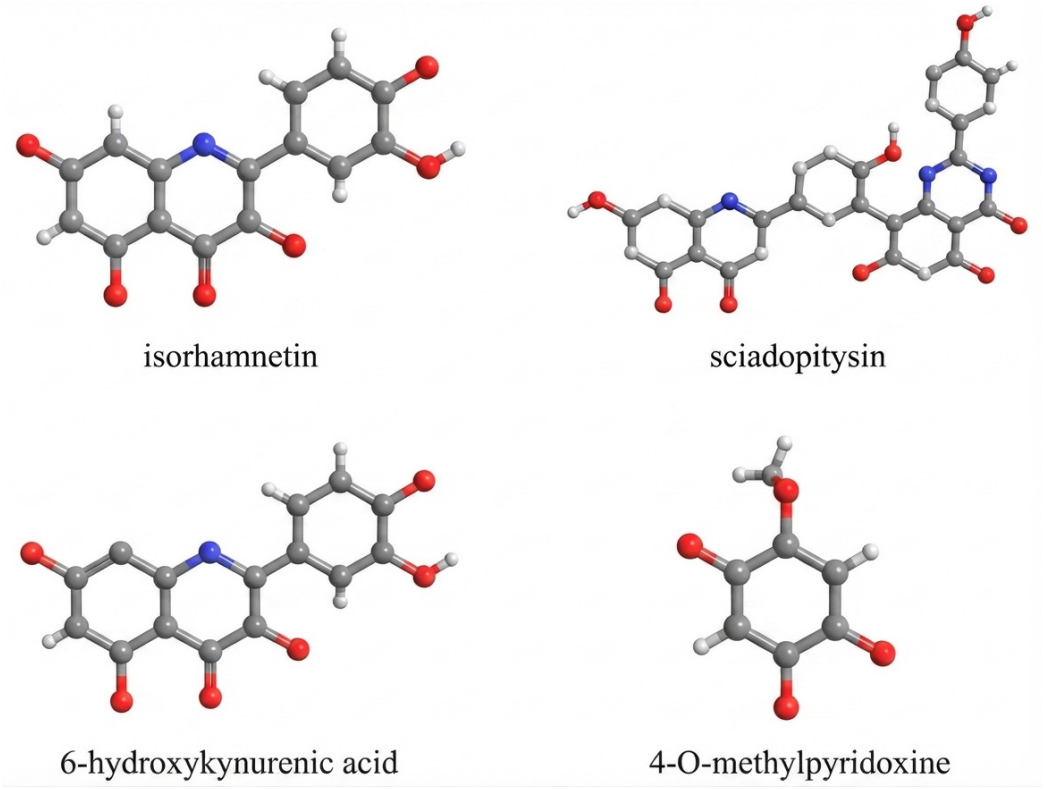

Figure 14. Chemical constituents of EGb.

5.2. Carrier Materials: A Key Pathway to Stimuli Responsiveness and Long-Term Inhibition Performance

Traditional admixed corrosion inhibitors, especially organic ones, may chemically react with cement hydration products during service. This not only causes premature consumption of inhibitors and attenuation of inhibition efficiency, but also interferes with the hydration process and microstructure of concrete, bringing adverse effects on its mechanical properties and durability.

To address the above issues, researchers have developed supported corrosion inhibitor systems by using cement-compatible carrier materials (microcapsules, LDHs, zeolites, etc.) to encapsulate active inhibiting components [65,151,152]. Benefiting from the unique structure and properties of carriers, supported inhibitors can intelligently respond to chloride ingress or concrete alkalinity reduction and release active components on demand.

This design helps alleviate the premature consumption and loss of inhibitors, which is beneficial for maintaining long-term corrosion protection performance. In addition, certain supported systems can provide extra functions such as chloride-ion immobilization and targeted migration.

Among various carrier materials, LDH is an anionic layered compound with a brucite-like structure, featuring excellent ion exchange capacity, structural memory effect, and thermal stability. Figure 15 illustrates the dynamic ion exchange process between inhibitor anions intercalated within the layered double hydroxide (LDH) interlayers and externally introduced chloride ions. By intercalating inhibiting components into the LDH interlayer to construct inhibitor-intercalated LDH (INT-LDH), the system can intelligently respond to aggressive anions such as Cl^- and SO_4^{2-} in concrete: it releases inhibiting components via ion exchange while adsorbing and immobilizing aggressive ions, achieving dual functions of corrosion protection and harmful ion fixation (Figure 15).

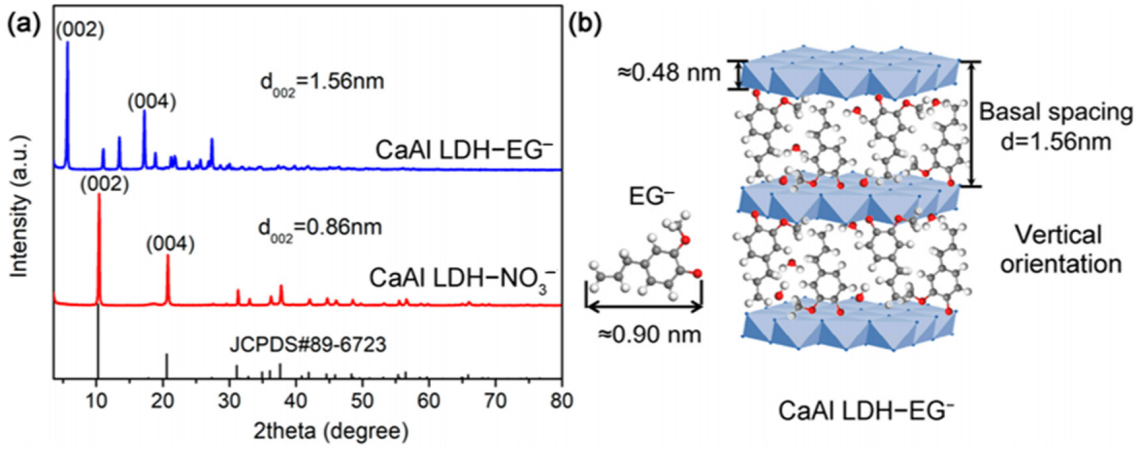

Figure 15. Structure and ion exchange mechanism of LDH. (**a**) XRD patterns of LDHs; and (**b**) diagram of EG^- in the interlayer space of LDH. Reprinted from Ref. [151].

LDH, a class of anionic layered compounds with a brucite-like structure, possesses excellent ion-exchange capacity, structural memory effect, and thermal stability, making them promising nanocontainers for plant-based corrosion inhibitors [153]. Liu et al. [154] synthesized CaAl-LDH intercalated with eugenol (EG)—a plant-based organic inhibitor extracted from *Cinnamomum verum* leaves—via a continuous hydrothermal method (Figure 15). As confirmed by XRD (Figure 15a), the successful intercalation of EG^- anions into the LDH interlayer gallery was evidenced by the shift in the (002) diffraction peak toward lower 2θ values, with the basal spacing expanding from 0.86 nm (CaAl-LDH-NO_3^-) to 1.56 nm (CaAl-LDH-EG^-); the EG^- anions adopt a vertical orientation within the interlayer space (Figure 15b). The loading amount of EG reached approximately 30 wt%, and about 80% of the intercalated EG was released within 4 h in simulated concrete pore solution containing 3.5% NaCl, demonstrating a rapid Cl^--stimuli-responsive release behavior. The underlying protection mechanism involves a dynamic anion-exchange process: externally invading Cl^- ions are exchanged with EG^- anions intercalated in the LDH interlayers, thereby simultaneously releasing the plant-based inhibitor to adsorb on the steel surface and immobilizing aggressive chloride ions within the LDH structure. Electrochemical results showed that, after 16 dry-wet cycles in 3.5% NaCl, the charge transfer resistance of steel-mortar specimens incorporated with LDH-EG (10^5–10^6 Ω·cm^2) was 3–4 orders of magnitude higher than that of the control (10^2–10^3 Ω·cm^2), with an inhibition efficiency exceeding 99%. This remarkable performance is attributed to the synergistic effect of LDH

pore-filling (reducing mortar permeability) and the sustained release of EG for long-term corrosion protection.

To date, various INT-LDH systems have been reported, including those intercalated with inorganic inhibitors and organic inhibitors, all of which exhibit excellent chloride-responsive inhibition performance. The structural characteristics and applicability of different carrier materials are compared in Table 2.

Table 2. Structural characteristics and applicability of typical INT-LDH systems.

Category	INT-LDH System	Intercalated Inhibitor Type	Applicable Medium	Typical Dosage	Reference
Inorganic inhibitor-intercalated LDH	MgAl-LDH-NO_2^-	Inorganic anodic inhibitor (nitrite)	SCP solution/mortar with Cl^- and SO_4^{2-}	1 g/100 mL	[155,156]
	CaAl-LDH-NO_3^-	Inorganic anion (nitrate)	SCP solution with Cl^-	1–2 wt.%	[157]
	CrO_4-LDH	Inorganic passivation inhibitor (chromate)	SCP solution with Cl^-	1 g/200 mL	[158]
Organic inhibitor-intercalated LDH	MgAl-LDH-pAB	Organic corrosion inhibitor (p-aminobenzoic acid)	Mortar	5–10 wt.%	[159,160]
	C_6H_5COO-LDH	Organic anodic inhibitor (benzoate)	SCP solution with Cl^-	1 g/200 mL	[158]
	MgAl-LDH-OH-PTL	Organic green corrosion inhibitor (phthalates)	SCP solution with Cl^- and CO_3^{2-}	20 g/L	[161]
Composite modified INT-LDH	SiO_2@LDH-NO_2^-	Inorganic anodic inhibitor (nitrite)	SCP solution with Cl^-	0.5 g/100 mL	[162]
	Sepiolite-supported MgAl-LDH	Inorganic anodic inhibitor (nitrite)	SCP solution with Cl^-	-	[66]
	Zeolite-LTA@MgAl-LDH-NO_3^-	Inorganic anion (nitrate, for ion exchange)	Saturated $Ca(OH)_2$ solution with Cl^-	1 g/100 mL	[163]

5.3. EGb-LDH Chloride-Immobilizing Controlled-Release Corrosion Inhibitor

On the basis of EGb active components and LDH carrier technology, constructing an EGb-LDH chloride-immobilizing controlled-release composite inhibitor is a valuable attempt to develop multi-functional plant-based corrosion inhibitors. This system integrates the green inhibition activity of EGb and the intelligent response performance of LDH, and is expected to address a persistent technical challenge of insufficient stability and single function of plant-based inhibitors.

Existing INT-LDH studies have provided clear technical ideas and theoretical foundations for the development of EGb-LDH, but its practical application still requires breakthroughs in several key scientific issues: the controllable preparation method of EGb-LDH, the formation and regulation mechanism of its microstructure, its chloride immobilization and controlled release characteristics, and the corresponding influencing factors. From the perspective of functional design, the core innovation of the EGb-LDH system is reflected in three aspects:

(1) **Potential environmental advantage:** The EGb components identified through theoretical screening, separation, and purification are used as the primary inhibiting constituents, which may provide a renewable and potentially lower-toxicity basis for the composite system. However, their environmental safety should be further verified through standardized toxicity, ecotoxicity, leaching, and life-cycle assessments.

(2) **Stability enhancement:** Intercalating EGb components into the LDH interlayer may reduce their direct exposure to the highly alkaline concrete pore environment, thereby improving the chemical stability and retention of plant-derived inhibitory constituents. This strategy is expected to mitigate, rather than completely eliminate, the possible deactivation of plant-based inhibitors during long-term service in alkaline media.

(3) **Dual-function chloride-responsive behavior:** Based on the chloride-responsive ion-exchange capability of LDH, the EGb-LDH composite system is designed to combine chloride ion immobilization with controlled inhibitor release. The released EGb components may contribute to the stabilization or repair of the passive film on steel, while LDH may reduce free chloride availability through ion exchange or adsorption. These coupled effects could improve the efficiency and durability of corrosion protection, although their long-term performance still requires validation under realistic concrete exposure conditions.

Systematic investigation of the EGb-LDH composite system may help address several important scientific and technical issues, including controllable preparation, performance evaluation, release behavior, corrosion-inhibition mechanism, and compatibility with cementitious materials. Such research could provide theoretical and experimental support for the development of plant-derived, long-lasting corrosion inhibitors for concrete structures exposed to aggressive environments. It may also offer useful data and mechanistic insights for the durability design of reinforced concrete structures with extended service life.

6. Perspective and Outlook

This paper reviews steel corrosion mechanisms, conventional corrosion inhibitor systems, and the latest advances in plant-based inhibitors for RC structures, covering their classification, performance evaluation, mechanisms, technical bottlenecks, and development strategies. The main conclusions are drawn as follows:

(1) Chloride ingress is a major factor governing durability deterioration in RC. By penetrating through pores and cracks, chloride ions depassivate reinforcing steel and trigger localized electrochemical corrosion, which may eventually result in cracking, spalling, and structural performance loss. Conventional inhibitor systems have respective merits and drawbacks, and new-generation inhibitors are increasingly being developed toward multifunctional, low-toxicity, and long-lasting systems.

(2) Plant-based corrosion inhibitors show considerable potential as sustainable alternatives to conventional inhibitors. Their corrosion protection is commonly attributed to synergistic mechanisms such as adsorption film formation, metal-ion complexation, antioxidative effects, and electrochemical regulation. The integrated system of electrochemical tests, multi-scale characterization, DFT/MD simulations, and machine learning provides multi-dimensional methodological support for active component screening, performance evaluation, and mechanism analysis.

(3) Composite modification is likely to be a key route for improving the engineering applicability of plant-based inhibitors. The EGb-LDH chloride-binding controlled-release concept illustrates the potential of combining active natural compounds with carrier-based stabilization and responsive release technologies. Future studies should therefore focus on active-component identification, green extraction, structural stabilization, and long-term service performance in chloride-containing environments.

(4) Standardization of extraction and compositional analysis represents a critical research priority. Future studies are encouraged to adopt more consistent protocols for extraction, purification, and characterization to enhance comparability across independent studies and better elucidate the links between plant extract composition and corrosion inhibition performance. Advanced quantitative analytical techniques, including

HPLC, GC-MS, and LC-MS/MS, should be more broadly applied where appropriate to systematically identify core active constituents and establish robust structure–activity relationships.

(5) Environmental safety profiles require standardized evaluation. While plant-derived inhibitors are widely regarded as environmentally benign, their overall environmental footprint is shaped by multiple factors across the full life cycle, including extraction processes, solvent selection, applied dosage, and potential leaching risks. Standardized assessments of toxicity, ecotoxicity, biodegradability, and life-cycle impacts are therefore warranted to robustly validate their eco-friendly attributes and support their practical engineering application.

Author Contributions: Conceptualization, D.S.; methodology, D.S. and X.Z.; software, G.W.; validation, G.W. and X.Z.; formal analysis, M.X. and X.Z.; investigation, C.H.; resources, D.S.; data curation, X.Z. and M.X.; writing—original draft preparation, M.X. and D.S.; writing—review and editing, C.H. and X.Z.; visualization, G.W. and C.H.; supervision, G.W., X.Z. and D.S.; project administration, X.Z. and D.S.; funding acquisition, G.W. and D.S. All authors have read and agreed to the published version of the manuscript.

Funding: The authors acknowledge the financial support from the National Natural Science Foundation of China (52278255) and the Fundamental Research Funds for the Central Universities (B260201073).

Data Availability Statement: No new data were created or analyzed in this study. Data sharing is not applicable to this article.

Conflicts of Interest: The authors declare no conflicts of interest.

References

1. Qu, F.; Li, W.; Dong, W.; Tam, V.W.Y.; Yu, T. Durability deterioration of concrete under marine environment from material to structure: A critical review. *J. Build. Eng.* **2021**, *35*, 102074. [CrossRef]
2. Rodrigues, R.; Gaboreau, S.; Gance, J.; Ignatiadis, I.; Betelu, S. Reinforced concrete structures: A review of corrosion mechanisms and advances in electrical methods for corrosion monitoring. *Constr. Build. Mater.* **2021**, *269*, 121240. [CrossRef]
3. Koushkbaghi, M.; Alipour, P.; Tahmouresi, B.; Mohseni, E.; Saradar, A.; Sarker, P.K. Influence of different monomer ratios and recycled concrete aggregate on mechanical properties and durability of geopolymer concretes. *Constr. Build. Mater.* **2019**, *205*, 519–528. [CrossRef]
4. Tang, S.W.; Yao, Y.; Andrade, C.; Li, Z.J. Recent durability studies on concrete structure. *Cem. Concr. Res.* **2015**, *78*, 143–154. [CrossRef]
5. Yonezawa, T.; Ashworth, V.; Procter, R.P.M. Pore solution composition and chloride effects on the corrosion of steel in concrete. *Corrosion* **1988**, *44*, 489–499. [CrossRef]
6. Yan, X.; Zhang, F.; Peng, S.; Yan, H.; Yang, M.; Duan, W.; Bao, X.; Chen, X.; Cui, H. Dual-path suppression of thermal and wetting-driven steel corrosion for marine structure. *Nat. Commun.* **2026**, *17*, 5471. [CrossRef] [PubMed]
7. Zhang, M.; Sun, S.; Liu, K.; Li, T.; Yang, H. Research on the critical chloride content of reinforcement corrosion in marine concrete—A review. *J. Build. Eng.* **2023**, *79*, 107838. [CrossRef]
8. Ren, M.; Wang, Z.; Aoki, H.; Takahashi, H.; Maekawa, K. Numerical investigation on chloride-induced macro-cell corrosion of steel fiber reinforced concrete. *Constr. Build. Mater.* **2024**, *455*, 139194. [CrossRef]
9. Feng, W.; Tarakbay, A.; Ali Memon, S.; Tang, W.; Cui, H. Methods of accelerating chloride-induced corrosion in steel-reinforced concrete: A comparative review. *Constr. Build. Mater.* **2021**, *289*, 123165. [CrossRef]
10. Stefanoni, M.; Angst, U.; Elsener, B. Corrosion rate of carbon steel in carbonated concrete—A critical review. *Cem. Concr. Res.* **2018**, *103*, 35–48. [CrossRef]
11. Liu, Y.; Zhou, X.; Guan, X.; Shi, J. Synergistic inhibition mechanism of phosphate and phytic acid on carbon steel in carbonated concrete pore solutions containing chlorides. *Corros. Sci.* **2022**, *208*, 110637. [CrossRef]
12. Angulo Ramirez, D.E.; Meira, G.R.; Quattrone, M.; John, V.M. A review on reinforcement corrosion propagation in carbonated concrete—Influence of material and environmental characteristics. *Cem. Concr. Compos.* **2023**, *140*, 105085. [CrossRef]
13. Wang, X.; Liu, J.; Jin, M.; Yan, Y.; Tang, J.; Jin, Z. A review of organic corrosion inhibitors for resistance under chloride attacks in reinforced concrete: Background, mechanisms and evaluation methods. *Constr. Build. Mater.* **2024**, *433*, 136583. [CrossRef]

14. Söylev, T.A.; Richardson, M.G. Corrosion inhibitors for steel in concrete: State-of-the-art report. *Constr. Build. Mater.* **2008**, *22*, 609–622. [CrossRef]
15. Bolzoni, F.; Brenna, A.; Ormellese, M. Recent advances in the use of inhibitors to prevent chloride-induced corrosion in reinforced concrete. *Cem. Concr. Res.* **2022**, *154*, 106719. [CrossRef]
16. Seneviratne, A.M.G.; Sergi, G.; Page, C.L. Performance characteristics of surface coatings applied to concrete for control of reinforcement corrosion. *Constr. Build. Mater.* **2000**, *14*, 55–59. [CrossRef]
17. Alamiery, A.; Shaker, L.M. Smart and green corrosion inhibitors: Mechanisms, computational tools, and sustainable protection strategies. *Mater. Chem. Phys.* **2026**, *348*, 131639. [CrossRef]
18. Hernández, E.F.; Cano-Barrita, P.F.d.J.; León-Martínez, F.M.; Torres-Acosta, A.A. Performance of cactus mucilage and brown seaweed extract as a steel corrosion inhibitor in chloride contaminated alkaline media. *Anti-Corros. Methods Mater.* **2017**, *64*, 529–539. [CrossRef]
19. Song, Z.; Donkor, S.; Zhang, Y.; Liu, Q.; Liu, Y.; Na, X.; Cai, H.; Kwesi Odoom, J. Adsorption and corrosion inhibition performance of rice bran extract on carbon steel in aqueous chloride solution: Experimental, computational and theoretical studies. *Constr. Build. Mater.* **2023**, *363*, 129801. [CrossRef]
20. Murungi, P.I.; Sulaimon, A.A. Ideal corrosion inhibitors: A review of plant extracts as corrosion inhibitors for metal surfaces. *Corros. Rev.* **2022**, *40*, 127–136. [CrossRef]
21. Casanova, L.; Ceriani, F.; Messinese, E.; Paterlini, L.; Beretta, S.; Bolzoni, F.M.; Brenna, A.; Diamanti, M.V.; Ormellese, M.; Pedeferri, M. Recent advances in the use of green corrosion inhibitors to prevent chloride-induced corrosion in reinforced concrete. *Materials* **2023**, *16*, 7462. [CrossRef] [PubMed]
22. Zomorodian, A.; Behnood, A. Review of corrosion inhibitors in reinforced concrete: Conventional and green materials. *Buildings* **2023**, *13*, 1170. [CrossRef]
23. Alhozaimy, A.; Hussain, R.R.; Al-Negheimish, A.; Ahmed, M.; Singh, D.D.N. Kinetics and mechanism of gallic acid as an ecofriendly corrosion inhibitor for steel rebars in mortar. *Sci. Rep.* **2024**, *14*, 31015. [CrossRef] [PubMed]
24. Wu, R.-J.; Xia, J.; Cheng, X.; Liu, K.-H.; Chen, K.-Y.; Liu, Q.-F.; Jin, W.-L. Effect of random aggregate distribution on chloride-induced corrosion morphology of steel in concrete. *Constr. Build. Mater.* **2022**, *322*, 126378. [CrossRef]
25. Taheri-Shakib, J.; Al-Mayah, A. Effect of corrosion pit distribution of rebar on pore, and crack characteristics in concrete. *Cem. Concr. Compos.* **2024**, *148*, 105476. [CrossRef]
26. Apostolopoulos, C.; Apostolopoulos, A.L.; Apostolopoulos, A. Engineering Assessment of Structural Deterioration and Preservation Challenges in a Corroded Reinforced Concrete Building Exposed to a Marine Environment. *Buildings* **2026**, *16*, 2997. [CrossRef]
27. James, A.; Bazarchi, E.; Chiniforush, A.A.; Panjebashi Aghdam, P.; Hosseini, M.R.; Akbarnezhad, A.; Martek, I.; Ghodoosi, F. Rebar corrosion detection, protection, and rehabilitation of reinforced concrete structures in coastal environments: A review. *Constr. Build. Mater.* **2019**, *224*, 1026–1039. [CrossRef]
28. Alexander, M.; Beushausen, H. Durability, service life prediction, and modelling for reinforced concrete structures—Review and critique. *Cem. Concr. Res.* **2019**, *122*, 17–29. [CrossRef]
29. Zhao, Y.; Dong, J.; Wu, Y.; Jin, W. Corrosion-induced concrete cracking model considering corrosion product-filled paste at the concrete/steel interface. *Constr. Build. Mater.* **2016**, *116*, 273–280. [CrossRef]
30. Cao, Y.; Gehlen, C.; Angst, U.; Wang, L.; Wang, Z.; Yao, Y. Critical chloride content in reinforced concrete—An updated review considering Chinese experience. *Cem. Concr. Res.* **2019**, *117*, 58–68. [CrossRef]
31. Yi, Y.; Zhu, D.; Guo, S.; Zhang, Z.; Shi, C. A review on the deterioration and approaches to enhance the durability of concrete in the marine environment. *Cem. Concr. Compos.* **2020**, *113*, 103695. [CrossRef]
32. Li, K.; Zhang, D.; Li, Q.; Fan, Z. Durability for concrete structures in marine environments of HZM project: Design, assessment and beyond. *Cem. Concr. Res.* **2019**, *115*, 545–558. [CrossRef]
33. Oware Sarfo, K.; Murkute, P.; Isgor, O.B.; Zhang, Y.; Tucker, J.; Árnadóttir, L. Density functional theory study of the initial stages of Cl-Induced degradation of α-Cr_2O_3 passive film. *J. Electrochem. Soc.* **2020**, *167*, 121508. [CrossRef]
34. Zhou, S.; Yan, Q.; Tang, C.; Mao, F.; Pu, J.; Macdonald, D.D. Effect of the chloride on passivity breakdown of Al-Zn-Mg alloy. *Corros. Sci.* **2020**, *163*, 108254. [CrossRef]
35. Zhou, Y.; Yu, Y.; Guo, W.; Xing, F.; Guo, M. Development of inorganic anticorrosive coatings for steel bars: Corrosion resistance testing and design. *Cem. Concr. Compos.* **2024**, *152*, 105612. [CrossRef]
36. Wang, D.; Wang, Y.; Ma, K.; Dai, C.; Wang, J.; Wang, J.; Pan, F. Portland cementitious coating with autogenerated oxide film and its anticorrosion behavior on magnesium alloy. *J. Mater. Sci. Technol.* **2024**, *176*, 99–111. [CrossRef]
37. Liu, Y.; Shi, J. Exploring a feasible inhibitor-coating protective system for corrosion protection of steel in mortar. *Cem. Concr. Compos.* **2025**, *161*, 106109. [CrossRef]
38. Liu, Y.; Guan, X.; Shi, J. Synergistic inhibition of molybdate and phytate on chloride-induced corrosion of carbon steel in simulated concrete pore solutions. *Cem. Concr. Compos.* **2024**, *145*, 105366. [CrossRef]

39. Uvida, M.C.; Trentin, A.; Harb, S.V.; Pulcinelli, S.H.; Santilli, C.V.; Hammer, P. Nanostructured poly(methyl methacrylate)–silica coatings for corrosion protection of reinforcing steel. *ACS Appl. Nano Mater.* **2022**, *5*, 2603–2615. [CrossRef]
40. Sajid, H.U.; Kiran, R.; Bajwa, D.S. Soy-protein and corn-derived polyol based coatings for corrosion mitigation in reinforced concrete. *Constr. Build. Mater.* **2022**, *319*, 126056. [CrossRef]
41. Ma, L.; Ren, C.; Wang, J.; Liu, T.; Yang, H.; Wang, Y.; Huang, Y.; Zhang, D. Self-reporting coatings for autonomous detection of coating damage and metal corrosion: A review. *Chem. Eng. J.* **2021**, *421*, 127854. [CrossRef]
42. Qian, H.; Mao, J.; Ye, S.; Xu, Z.; Chen, S.; Liu, Y.; Yan, D. Coated rebars for reinforced concrete structures: A review. *J. Build. Eng.* **2025**, *109*, 113000. [CrossRef]
43. Meng, F.; Chen, Y.; Chi, J.; Wang, H.; Wang, F.; Liu, L. Lifetime prediction of epoxy coating using convolutional neural networks and post processing image recognition methods. *npj Mater. Degrad.* **2024**, *8*, 114. [CrossRef]
44. Yoo, D.-Y.; Oh, T.; Banthia, N. Nanomaterials in ultra-high-performance concrete (UHPC)—A review. *Cem. Concr. Compos.* **2022**, *134*, 104730. [CrossRef]
45. Zeng, J.-J.; Hao, Z.-H.; Sun, H.-Q.; Zeng, W.-B.; Fan, T.-H.; Zhuge, Y. Durability assessment of ultra-high-performance concrete (UHPC) and FRP grid-reinforced UHPC plates under marine environments. *Eng. Struct.* **2025**, *323*, 119313. [CrossRef]
46. Reda, M.M.; Shrive, N.G.; Gillott, J.E. Microstructural investigation of innovative UHPC. *Cem. Concr. Res.* **1999**, *29*, 323–329. [CrossRef]
47. Qiu, M.; Shao, X.; Yan, B.; Zhu, Y.; Chen, Y. Flexural behavior of UHPC joints for precast UHPC deck slabs. *Eng. Struct.* **2022**, *251*, 113422. [CrossRef]
48. Du, J.; Meng, W.; Khayat, K.H.; Bao, Y.; Guo, P.; Lyu, Z.; Abu-obeidah, A.; Nassif, H.; Wang, H. New development of ultra-high-performance concrete (UHPC). *Compos. Part B Eng.* **2021**, *224*, 109220. [CrossRef]
49. Xia, J.; Li, T.; Fang, J.-X.; Jin, W.-L. Numerical simulation of steel corrosion in chloride contaminated concrete. *Constr. Build. Mater.* **2019**, *228*, 116745. [CrossRef]
50. Wang, Y.-Q.; Kong, G.; Che, C.-S.; Zhang, B. Inhibitive effect of sodium molybdate on the corrosion behavior of galvanized steel in simulated concrete pore solution. *Constr. Build. Mater.* **2018**, *162*, 383–392. [CrossRef]
51. Shi, J.; Wu, M.; Ming, J. In-depth insight into the role of molybdate in corrosion resistance of reinforcing steel in chloride-contaminated mortars. *Cem. Concr. Compos.* **2022**, *132*, 104628. [CrossRef]
52. Mohamed, A.; Visco, D.P.; Bastidas, D.M. Effect of cations on the activity coefficient of NO_2^-/NO_3^- corrosion inhibitors in simulated concrete pore solution: An electrochemical thermodynamics study. *Corros. Sci.* **2022**, *206*, 110476. [CrossRef]
53. Ming, J.; Zhou, X.; Zuo, H.; Jiang, L.; Zou, Y.; Shi, J. Effects of stray current and silicate ions on electrochemical behavior of a high-strength prestressing steel in simulated concrete pore solutions. *Corros. Sci.* **2022**, *197*, 110083. [CrossRef]
54. Liu, C.; Sridhar, N. The effects of chloride, nitrate, and nitrite on the localized corrosion of carbon steel in simulated concrete pore solutions. *Corrosion* **2021**, *77*, 350–367. [CrossRef] [PubMed]
55. Chen, Z.; Ye, H. Sequestration and release of nitrite and nitrate in alkali-activated slag: A route toward smart corrosion control. *Cem. Concr. Res.* **2021**, *143*, 106398. [CrossRef]
56. Wu, M.; Ma, H.; Shi, J. Beneficial and detrimental effects of molybdate as an inhibitor on reinforcing steels in saturated $Ca(OH)_2$ solution: Spontaneous passivation. *Cem. Concr. Compos.* **2021**, *116*, 103887. [CrossRef]
57. Shi, J.; Sun, W.; Jiang, J.; Zhang, Y. Influence of chloride concentration and pre-passivation on the pitting corrosion resistance of low-alloy reinforcing steel in simulated concrete pore solution. *Constr. Build. Mater.* **2016**, *111*, 805–813. [CrossRef]
58. Rivera-Corral, J.O.; Fajardo, G.; Arliguie, G.; Orozco-Cruz, R.; Deby, F.; Valdez, P. Corrosion behavior of steel reinforcement bars embedded in concrete exposed to chlorides: Effect of surface finish. *Constr. Build. Mater.* **2017**, *147*, 815–826. [CrossRef]
59. Mohagheghi, A.; Arefinia, R. Corrosion inhibition of carbon steel by dipotassium hydrogen phosphate in alkaline solutions with low chloride contamination. *Constr. Build. Mater.* **2018**, *187*, 760–772. [CrossRef]
60. Pachón-Montaño, A.; Sánchez-Montero, J.; Andrade, C.; Fullea, J.; Moreno, E.; Matres, V. Threshold concentration of chlorides in concrete for stainless steel reinforcement: Classic austenitic and new duplex stainless steel. *Constr. Build. Mater.* **2018**, *186*, 495–502. [CrossRef]
61. Zhang, W.; François, R.; Cai, Y.; Charron, J.-P.; Yu, L. Influence of artificial cracks and interfacial defects on the corrosion behavior of steel in concrete during corrosion initiation under a chloride environment. *Constr. Build. Mater.* **2020**, *253*, 119165. [CrossRef]
62. Zhou, X.; Ma, Q.; Li, M.; Liu, Y.; Shi, J. Inhibition mechanism of carboxylate-based inhibitors on HRB400E steel in simulated concrete pore solutions: A comprehensive consideration of passivation behavior and corrosion resistance. *Cem. Concr. Compos.* **2025**, *160*, 106063. [CrossRef]
63. Zhou, X.; Geng, Z.; Shi, J. Dual effects of phytic acid on reinforced low-carbon mortar: Dealkalization of red mud and improvement of corrosion resistance. *Cem. Concr. Compos.* **2025**, *164*, 106274. [CrossRef]
64. Zhang, W.; Zheng, Q.; Ashour, A.; Han, B. Self-healing cement concrete composites for resilient infrastructures: A review. *Compos. Part B Eng.* **2020**, *189*, 107892. [CrossRef]

65. Dong, B.; Ding, W.; Qin, S.; Han, N.; Fang, G.; Liu, Y.; Xing, F.; Hong, S. Chemical self-healing system with novel microcapsules for corrosion inhibition of rebar in concrete. *Cem. Concr. Compos.* **2018**, *85*, 83–91. [CrossRef]
66. Ma, G.; Xu, J.; Wang, Z. Inhibitive effect of sepiolite-supported MgAl-LDH on chloride-induced corrosion of steel in simulated concrete pore solution. *Corros. Sci.* **2023**, *225*, 111571. [CrossRef]
67. Ma, C.; Wang, X.; Tian, W.; Zou, F.; Zhong, Y.; Guo, G.; Zhang, C. A biomimetic protection system for reinforced concrete based on industrial solid waste and bio-based materials: Synergistic anti-corrosion microcapsules with dual functions of self-healing and chelation. *Cem. Concr. Compos.* **2026**, *173*, 106694. [CrossRef]
68. An, H.; Ngendabanyikwa, D.; Meng, G.; Wang, Y.; Wang, J.; Liu, B.; Wang, F. A Novel Self-Healing Conversion Film Formed on Rebar in Solution Containing Cerium and Molybdenum Ions. *J. Electrochem. Soc.* **2022**, *169*, 011501. [CrossRef]
69. Pradipta, I.; Kong, D.; Tan, J.B.L. Natural organic antioxidants from green tea inhibit corrosion of steel reinforcing bars embedded in mortar. *Constr. Build. Mater.* **2019**, *227*, 117058. [CrossRef]
70. Ding, C.; Liu, J.; Zhang, X.; Wang, J.; Li, L.; Fu, K.; Chen, S. Corrosion dynamics of low carbon steel in salt spray environment. *Prot. Met. Phys. Chem. Surf.* **2023**, *59*, 729–735. [CrossRef]
71. Liu, Q.; Song, Z.; Han, H.; Donkor, S.; Jiang, L.; Wang, W.; Chu, H. A novel green reinforcement corrosion inhibitor extracted from waste Platanus acerifolia leaves. *Constr. Build. Mater.* **2020**, *260*, 119695. [CrossRef]
72. Anitha, R.; Chitra, S.; Hemapriya, V.; Chung, I.-M.; Kim, S.-H.; Prabakaran, M. Implications of eco-addition inhibitor to mitigate corrosion in reinforced steel embedded in concrete. *Constr. Build. Mater.* **2019**, *213*, 246–256. [CrossRef]
73. Chaieb, K.; Hajlaoui, H.; Zmantar, T.; Kahla-Nakbi, A.B.; Rouabhia, M.; Mahdouani, K.; Bakhrouf, A. The chemical composition and biological activity of clove essential oil, *Eugenia caryophyllata* (*Syzigium aromaticum* L. Myrtaceae): A short review. *Phytother. Res.* **2007**, *21*, 501–506. [CrossRef] [PubMed]
74. Biswas, K.; Chattopadhyay, I.; Banerjee, R.K.; Bandyopadhyay, U. Biological activities and medicinal properties of neem (*Azadirachta indica*). *Curr. Sci.* **2002**, *82*, 1336–1345.
75. Diamanti, M.V.; Pérez Rosales, E.A.; Raffaini, G.; Ganazzoli, F.; Brenna, A.; Pedeferri, M.; Ormellese, M. Molecular modelling and electrochemical evaluation of organic inhibitors in concrete. *Corros. Sci.* **2015**, *100*, 231–241. [CrossRef]
76. Zhang, Y.; Xu, Q.; Sun, M.; Xiong, C.; Wang, P.; Chen, Z.; Sun, G.; Guan, J.; Ding, Z.; Li, M.; et al. Insights into vitamin B3, B6 and C as inhibitor of steel reinforcement: A DFT + U study. *Constr. Build. Mater.* **2021**, *294*, 123571. [CrossRef]
77. Torres, P.; Osaki, S.; Silveira, E.; dos Santos, D.Y.A.C.; Chow, F. Comprehensive evaluation of Folin-Ciocalteu assay for total phenolic quantification in algae (Chlorophyta, Phaeophyceae, and Rhodophyta). *Algal Res.* **2024**, *80*, 103503. [CrossRef]
78. Duvigneau, S.; Kettner, A.; Carius, L.; Griehl, C.; Findeisen, R.; Kienle, A. Fast, inexpensive, and reliable HPLC method to determine monomer fractions in poly(3-hydroxybutyrate-co-3-hydroxyvalerate). *Appl. Microbiol. Biotechnol.* **2021**, *105*, 4743–4749. [CrossRef] [PubMed]
79. Mondello, L.; Cordero, C.; Janssen, H.-G.; Synovec, R.E.; Zoccali, M.; Tranchida, P.Q. Comprehensive two-dimensional gas chromatography–mass spectrometry. *Nat. Rev. Methods Primers* **2025**, *5*, 7. [CrossRef]
80. Yang, F.; Cui, H.; Wang, C.; Wang, Y.; Zhu, W.; Deng, H.; Liu, S.; Bian, Z.; Lu, J.; Tang, G.; et al. Comparison of supercritical fluid chromatography–tandem mass spectrometry and liquid chromatography–tandem mass spectrometry for the stereoselective analysis of chlorfenvinphos and dimethylvinphos in tobacco. *J. Sep. Sci.* **2023**, *46*, 2300449. [CrossRef] [PubMed]
81. *ASTM B117-26*; Standard Practice for Operating Salt Spray (Fog) Apparatus. ASTM International: West Conshohocken, PA, USA, 2026.
82. *ASTM G85-19*; Standard Practice for Modified Salt Spray (Fog) Testing. ASTM International: West Conshohocken, PA, USA, 2019.
83. *ASTM G109-23*; Standard Test Methods for Determining Effects of Chemical Admixtures on Corrosion of Embedded Steel Reinforcement in Concrete Exposed to Chloride Environments. ASTM International: West Conshohocken, PA, USA, 2023.
84. Hansson, C.M.; Poursaee, A.; Laurent, A. Macrocell and microcell corrosion of steel in ordinary Portland cement and high performance concretes. *Cem. Concr. Res.* **2006**, *36*, 2098–2102. [CrossRef]
85. Ming, J.; Shi, J. Mechanism of enhanced corrosion resistance of 9CrMo rebar in low-carbon mortar: Unique distribution and interfacial evolution of mill scale and corrosion products. *J. Mater. Sci. Technol.* **2026**, *275*, 312–325. [CrossRef]
86. Salman, M.; Sikandar, M.A.; Nasir, H.; Waseem, M.; Iqbal, S. Protection against reinforcement corrosion using various hydroxy acid-based rust converters: Tests in mortar medium. *Eur. J. Environ. Civ. Eng.* **2022**, *26*, 4130–4145. [CrossRef]
87. Yao, N.; Zhou, X.; Liu, Y.; Shi, J. Synergistic effect of red mud and fly ash on passivation and corrosion resistance of 304 stainless steel in alkaline concrete pore solutions. *Cem. Concr. Compos.* **2022**, *132*, 104637. [CrossRef]
88. *ASTM C876-22b*; Standard Test Method for Corrosion Potentials of Uncoated Reinforcing Steel in Concrete. ASTM International: West Conshohocken, PA, USA, 2022.
89. Lin, B.; Zuo, Y. Corrosion inhibition of carboxylate inhibitors with different alkylene chain lengths on carbon steel in an alkaline solution. *RSC Adv.* **2019**, *9*, 7065–7077. [CrossRef] [PubMed]
90. Blanco, G.; Bautista, A.; Takenouti, H. EIS study of passivation of austenitic and duplex stainless steels reinforcements in simulated pore solutions. *Cem. Concr. Compos.* **2006**, *28*, 212–219. [CrossRef]

91. Boissy, C.; Alemany-Dumont, C.; Normand, B. EIS evaluation of steady-state characteristic of 316L stainless steel passive film grown in acidic solution. *Electrochem. Commun.* **2013**, *26*, 10–12. [CrossRef]
92. Xu, P.; Zhou, J.; Li, G.; Wang, P.; Wang, P.; Li, F.; Zhang, B.; Chi, H. Corrosion inhibition efficiency of compound nitrite with D-sodium gluconate on carbon steel in simulated concrete pore solution. *Constr. Build. Mater.* **2021**, *288*, 123101. [CrossRef]
93. Zhao, Y.; Chen, Y.; Li, X.; Chen, D.; Wu, M. The use of TEA·H3PO4 and TEA·C18H30O3S as eco-friendly corrosion inhibitors in cementitious materials: An experimental and theoretical study. *Cem. Concr. Res.* **2023**, *165*, 107073. [CrossRef]
94. Feng, G.; Jin, Z.; Jiang, Y.; Wang, X.; Zhu, D. Localized corrosion propagation of steel in cracked mortar and long-term corrosion of steel reinforcement in cracked concrete in seawater environment. *Corros. Sci.* **2024**, *228*, 111793. [CrossRef]
95. Maachi, B.; Pirri, C.; Mehdaoui, A.; Hakiki, N.E.; Bubendorff, J.L. Atomic force microscopy, scanning kelvin probe force microscopy and magnetic measurements on thermally oxidized AISI 304 and AISI 316 stainless steels. *Corros. Sci.* **2011**, *53*, 984–991. [CrossRef]
96. Xu, J.; Wei, J.; Ma, G.; Tan, Q. Effect of MgAl-NO_2 LDHs inhibitor on steel corrosion in chloride-free and contaminated simulated carbonated concrete pore solutions. *Corros. Sci.* **2020**, *176*, 108940. [CrossRef]
97. Bernachy-Barbe, F.; Sayari, T.; Dewynter-Marty, V.; L'Hostis, V. Using X-ray microtomography to study the initiation of chloride-induced reinforcement corrosion in cracked concrete. *Constr. Build. Mater.* **2020**, *259*, 119574. [CrossRef]
98. Wan, H.; Wang, Y.; Zhao, Y. In-situ Raman spectroelectrochemistry for characterization of steel corrosion products in simulated concrete pore solution. *J. Build. Eng.* **2025**, *111*, 113098. [CrossRef]
99. Chen, H.; Qin, Z.; He, M.; Liu, Y.; Wu, Z. Application of electrochemical atomic force microscopy (EC-AFM) in the corrosion study of metallic materials. *Materials* **2020**, *13*, 668. [CrossRef] [PubMed]
100. Maurice, V.; Marcus, P. Progress in corrosion science at atomic and nanometric scales. *Prog. Mater. Sci.* **2018**, *95*, 132–171. [CrossRef]
101. Morwal, T.; Bansal, T.; Azam, A.; Talakokula, V.; Jothi Saravanan, T. Exploring chloride-induced corrosion in reinforced concrete structures through embedded piezo sensor technology: An experimental and numerical study. *Smart Mater. Struct.* **2024**, *33*, 035039. [CrossRef]
102. Quadri, T.W.; Olasunkanmi, L.O.; Akpan, E.D.; Fayemi, O.E.; Lee, H.-S.; Lgaz, H.; Verma, C.; Guo, L.; Kaya, S.; Ebenso, E.E. Development of QSAR-based (MLR/ANN) predictive models for effective design of pyridazine corrosion inhibitors. *Mater. Today Commun.* **2022**, *30*, 103163. [CrossRef]
103. Liu, Y.; Guo, Y.; Wu, W.; Xiong, Y.; Sun, C.; Yuan, L.; Li, M. A machine learning-based QSAR model for benzimidazole derivatives as corrosion inhibitors by incorporating comprehensive feature selection. *Interdiscip. Sci. Comput. Life Sci.* **2019**, *11*, 738–747. [CrossRef] [PubMed]
104. Marhamati, F.; Mahdavian, M.; Bazgir, S. Corrosion mitigation of mild steel in hydrochloric acid solution using grape seed extract. *Sci. Rep.* **2021**, *11*, 18374. [CrossRef] [PubMed]
105. Deng, S.; Li, X. Inhibition by Ginkgo leaves extract of the corrosion of steel in HCl and H_2SO_4 solutions. *Corros. Sci.* **2012**, *55*, 407–415. [CrossRef]
106. Kaushik, N.P.; Rao, P.; Kedimar, N.; Rao, S.A. Grape seed extract as an environment-friendly green inhibitor for corrosion of mild steel in 1 M sulfamic acid. *J. Mater. Eng. Perform.* **2024**, *33*, 10885–10894. [CrossRef]
107. Hidalgo, J.; Hidalgo, L.; Serrano Aguiar, C.D.; García Madroñero, D.B.; Galambos, I.; Vilasó-Cadre, J.E.; Reyes-Domínguez, I.A.; Brânzanic, A.M.V.; Ignat, N.; Turdean, G.L. Study of *Caesalpinia spinosa* extracts as green corrosion inhibitor for mild steel. *Langmuir* **2025**, *41*, 9406–9421. [CrossRef] [PubMed]
108. Rabizadeh, T. Evaluating the performance of corn peptone in preventing the corrosion of mild steel immersed in HCl. *Mater. Corros.* **2024**, *75*, 1142–1154. [CrossRef]
109. Li, Y.; Guo, Z.; Zhi, H.; Qiang, Y.; Liu, X.; Zhang, Y.; Wan, Y.; Xiang, T.; Li, X. Experimental and computational exploration of the biodegradable platanus acerifolia leaf extract against mild steel corrosion in hydrochloric acid. *J. Mater. Res. Technol.* **2024**, *30*, 7830–7842. [CrossRef]
110. Singh, A.; Ansari, K.R.; AbdelRahim, S.K.; Ali, I.H.; El Ibrahimi, B.; Alanazi, A.K.; Younas, M.; Lin, Y. Potential application of *Ginkgo biloba* extract as a green corrosion inhibitor for carbon steel reinforcement in chloride-polluted simulated concrete pore solution. *Process Saf. Environ. Prot.* **2024**, *186*, 819–832. [CrossRef]
111. Raghavendra, N.; Hublikar, L.V.; Patil, S.M.; Ganiger, P.J.; Bhinge, A.S. Efficiency of sapota leaf extract against aluminium corrosion in a 3 M sodium hydroxide hostile fluid atmosphere: A green and sustainable approach. *Bull. Mater. Sci.* **2019**, *42*, 226. [CrossRef]
112. Zhang, Z.; Ba, H.; Wu, Z. Sustainable corrosion inhibitor for steel in simulated concrete pore solution by maize gluten meal extract: Electrochemical and adsorption behavior studies. *Constr. Build. Mater.* **2019**, *227*, 117080. [CrossRef]
113. Abod, B.M.; Al-Alawy, R.M.; Khadom, A.A.; Kamar, F.H. Experimental and theoretical studies for tobacco leaf extract as an eco-friendly inhibitor for steel in saline water. *J. Bio-Tribo-Corros.* **2019**, *5*, 75. [CrossRef]

114. Song, Z.; Liu, L.; Guo, M.-Z.; Cai, H.; Liu, Q.; Donkor, S.; Zhao, H. Inhibition performance of extract reinforcement corrosion inhibitor from waste *Platanus acerifolia* leaves in simulated concrete pore solution. *Case Stud. Constr. Mater.* **2024**, *20*, e02992. [CrossRef]
115. Singh, J.K.; Mandal, S.; Lee, H.-S.; Yang, H.-M. Effect of chloride ions concentrations to breakdown the passive film on rebar surface exposed to L-arginine containing pore solution. *Materials* **2021**, *14*, 5693. [CrossRef] [PubMed]
116. Ben Harb, M.; Abubshait, S.; Etteyeb, N.; Kamoun, M.; Dhouib, A. Olive leaf extract as a green corrosion inhibitor of reinforced concrete contaminated with seawater. *Arab. J. Chem.* **2020**, *13*, 4846–4856. [CrossRef]
117. Zhang, Z.; Yang, B.; Tai, B.; Zhu, Y. Effect of maize gluten meal extract as natural corrosion inhibitor on steel in mortar corroded by chloride. *J. Build. Eng.* **2022**, *62*, 105394. [CrossRef]
118. Asaad, M.A.; Ismail, M.; Tahir, M.M.; Huseien, G.F.; Raja, P.B.; Asmara, Y.P. Enhanced corrosion resistance of reinforced concrete: Role of emerging eco-friendly *Elaeis guineensis*/silver nanoparticles inhibitor. *Constr. Build. Mater.* **2018**, *188*, 555–568. [CrossRef]
119. Huang, L.; Chen, W.-Q.; Wang, S.-S.; Zhao, Q.; Li, H.-J.; Wu, Y.-C. Starch, cellulose and plant extracts as green inhibitors of metal corrosion: A review. *Environ. Chem. Lett.* **2022**, *20*, 3235–3264. [CrossRef]
120. Verma, C.; Alfantazi, A.; Quraishi, M.A.; Rhee, K.Y. Are extracts really green substitutes for traditional toxic corrosion inhibitors? Challenges beyond origin and availability. *Sustain. Chem. Pharm.* **2023**, *31*, 100943. [CrossRef]
121. Holla, B.R.; Mahesh, R.; Manjunath, H.R.; Anjanapura, V.R. Plant extracts as green corrosion inhibitors for different kinds of steel: A review. *Heliyon* **2024**, *10*, e33748. [CrossRef] [PubMed]
122. Sesia, R.; Spriano, S.; Sangermano, M.; Ferraris, S. Natural polyphenols and the corrosion protection of steel: Recent advances and future perspectives for green and promising strategies. *Metals* **2023**, *13*, 1070. [CrossRef]
123. Pradipta, I.; Kong, D.; Tan, J.B.L. Natural organic antioxidants from green tea form a protective layer to inhibit corrosion of steel reinforcing bars embedded in mortar. *Constr. Build. Mater.* **2019**, *221*, 351–362. [CrossRef]
124. Jia, M.; Hu, P.; Gong, Z.; Sun, J.; Cui, Y.; Hu, D.; Hu, G. Corrosion inhibition and rust conversion of catechin on archaeological iron of Nanhai I. *Metals* **2022**, *12*, 714. [CrossRef]
125. Zhang, W.; Nie, B.; Wang, M.; Shi, S.; Gong, L.; Gong, W.; Pang, H.; Liu, X.; Li, B.; Feng, Y.; et al. Chemically modified resveratrol as green corrosion inhibitor for Q235 steel: Electrochemical, SEM, UV and DFT studies. *J. Mol. Liq.* **2021**, *343*, 117672. [CrossRef]
126. Lgaz, H.; Lee, H.-s. Computational exploration of phenolic compounds in corrosion inhibition: A case study of hydroxytyrosol and tyrosol. *Materials* **2023**, *16*, 6159. [CrossRef] [PubMed]
127. Liu, Y.; Shi, J. Corrosion resistance of carbon steel in alkaline concrete pore solutions containing phytate and chloride ions. *Corros. Sci.* **2022**, *205*, 110451. [CrossRef]
128. Cao, F.; Wei, J.; Dong, J.; Ke, W. The corrosion inhibition effect of phytic acid on 20SiMn steel in saturated $Ca(OH)_2$ solution with 1 mol L^{-1} NaCl. *Corros. Eng. Sci. Technol.* **2018**, *53*, 283–292. [CrossRef]
129. Paulson Maliekkal, B.; Kakkassery, J.T.; Palayoor, V.R. Efficacies of sodium nitrite and sodium citrateâzinc acetate mixture to inhibit steel rebar corrosion in simulated concrete interstitial solution contaminated with NaCl. *Int. J. Ind. Chem.* **2023**, *9*, 105–114. [CrossRef]
130. Chan-Rosado, G.; Pech-Canul, M.A. Influence of native oxide film age on the passivation of carbon steel in neutral aqueous solutions with a dicarboxylic acid. *Corros. Sci.* **2019**, *153*, 19–31. [CrossRef]
131. Lu, Z.; Lei, Z.; Zafar, M.N. Synthesis and performance characterization of an efficient environmental-friendly *Sapindus mukorossi* saponins based hybrid coal dust suppressant. *J. Clean. Prod.* **2021**, *306*, 127261. [CrossRef]
132. Tu, S.; Jiang, J.; Li, P.; Li, R.; Tang, Q. *Gleditsia sinensic* extract as green corrosion inhibitor for N80 steel in 1 M HCl. *J. Mol. Struct.* **2025**, *1321*, 139890. [CrossRef]
133. Kurtay, M.; Gerengi, H.; Chidiebere, A.; Yıldız, M. Corrosion inhibition of reinforcement steel in mixture water by caffeine and L-arginine. *J. Adhes. Sci. Technol.* **2022**, *36*, 134–167. [CrossRef]
134. Jiang, M.; Liu, X.; Hu, X.; Li, S.; Xu, Y.; Li, X.; Lu, L.; Xia, C.; Liu, X.; Wang, Z.; et al. Novel eco-friendly inhibitor for mild steel in simulated concrete pore solution: Experimental and theoretical analysis. *Chem. Eng. J.* **2025**, *525*, 170606. [CrossRef]
135. Zhang, Z.; Liu, Y.; Zhu, Y.; Shen, P. Corrosion inhibition performance and mechanism of glutenin on reinforcing steel in carbonated concrete pore solution: Experimental and theoretical studies. *J. Build. Eng.* **2025**, *113*, 114104. [CrossRef]
136. Sattari, R.; Khayati, G.R.; Darezereshki, E. Experimental and computational study of corrosion protection of carbon steel by *Lavandula angustifolia* extract–Zn(II) hybrid system in saline solution. *Sci. Rep.* **2026**, *16*, 22351. [CrossRef] [PubMed]
137. Mussey, B.K.; Akoto, R.N.A.; Damoah, L.N.W. Synergistic corrosion inhibition of steel reinforcement in concrete using calcined clay pozzolan and Acacia leaf extract. *Cogent Eng.* **2026**, *13*, 2696621. [CrossRef]
138. Boschmann Käthler, C.; Poulsen, S.L.; Sørensen, H.E.; Angst, U.M. Investigations of accelerated methods for determination of chloride threshold values for reinforcement corrosion in concrete. *Sustain. Resilient Infrastruct.* **2023**, *8*, 197–208. [CrossRef]
139. Liu, Q.-f. Progress and research challenges in concrete durability: Ionic transport, electrochemical rehabilitation and service life prediction. *RILEM Tech. Lett.* **2022**, *7*, 98–111. [CrossRef]

140. Young, J.F. A review of the mechanisms of set-retardation in portland cement pastes containing organic admixtures. *Cem. Concr. Res.* **1972**, *2*, 415–433. [CrossRef]
141. Gao, Y.; Luo, J.; Zhu, X.; Zhang, J.; Fan, K.; Ma, M. A review on the effect of organic admixtures containing different functional groups on the hydration behaviors of Portland cement. *Rev. Inorg. Chem.* **2026**, *46*, 197–216. [CrossRef]
142. Bishop, M.; Barron, A.R. Cement hydration inhibition with sucrose, tartaric acid, and lignosulfonate: Analytical and spectroscopic study. *Ind. Eng. Chem. Res.* **2006**, *45*, 7042–7049. [CrossRef]
143. Zingg, A.; Holzer, L.; Kaech, A.; Winnefeld, F.; Pakusch, J.; Becker, S.; Gauckler, L. The microstructure of dispersed and non-dispersed fresh cement pastes—New insight by cryo-microscopy. *Cem. Concr. Res.* **2008**, *38*, 522–529. [CrossRef]
144. Plank, J.; Hirsch, C. Impact of zeta potential of early cement hydration phases on superplasticizer adsorption. *Cem. Concr. Res.* **2007**, *37*, 537–542. [CrossRef]
145. Flatt, R.J.; Schober, I.; Raphael, E.; Plassard, C.d.; Lesniewska, E. Conformation of adsorbed comb copolymer dispersants. *Langmuir* **2008**, *25*, 845–855. [CrossRef] [PubMed]
146. Ormellese, M.; Berra, M.; Bolzoni, F.; Pastore, T. Corrosion inhibitors for chlorides induced corrosion in reinforced concrete structures. *Cem. Concr. Res.* **2006**, *36*, 536–547. [CrossRef]
147. Berke, N.S.; Hicks, M.C. Predicting long-term durability of steel reinforced concrete with calcium nitrite corrosion inhibitor. *Cem. Concr. Compos.* **2004**, *26*, 191–198. [CrossRef]
148. Montes, P.; Bremner, T.W.; Lister, D.H. Influence of calcium nitrite inhibitor and crack width on corrosion of steel in high performance concrete subjected to a simulated marine environment. *Cem. Concr. Compos.* **2004**, *26*, 243–253. [CrossRef]
149. Ann, K.Y.; Jung, H.S.; Kim, H.S.; Kim, S.S.; Moon, H.Y. Effect of calcium nitrite-based corrosion inhibitor in preventing corrosion of embedded steel in concrete. *Cem. Concr. Res.* **2006**, *36*, 530–535. [CrossRef]
150. Qiang, Y.; Zhang, S.; Tan, B.; Chen, S. Evaluation of Ginkgo leaf extract as an eco-friendly corrosion inhibitor of X70 steel in HCl solution. *Corros. Sci.* **2018**, *133*, 6–16. [CrossRef]
151. Yang, H.; Li, W.; Liu, X.; Liu, A.; Hang, P.; Ding, R.; Li, T.; Zhang, Y.; Wang, W.; Xiong, C. Preparation of corrosion inhibitor loaded zeolites and corrosion resistance of carbon steel in simulated concrete pore solution. *Constr. Build. Mater.* **2019**, *225*, 90–98. [CrossRef]
152. Hong, S.; Qin, S.; Liu, Z.; Liu, M.; Zhang, Y.; Dong, B. Enhanced corrosion resistance and applicability of Mg/Al-CO_3^{2-} layered double hydroxide film on Q235 steel substrate. *Constr. Build. Mater.* **2021**, *276*, 122259. [CrossRef]
153. Yang, H.; Xiong, C.; Liu, X.; Liu, A.; Li, T.; Ding, R.; Shah, S.P.; Li, W. Application of layered double hydroxides (LDHs) in corrosion resistance of reinforced concrete-state of the art. *Constr. Build. Mater.* **2021**, *307*, 124991. [CrossRef]
154. Liu, A.; Gu, H.; Geng, Y.; Wang, P.; Gao, S.; Li, S. Hydrothermal Synthesis of CaAl-LDH Intercalating with Eugenol and Its Corrosion Protection Performances for Reinforcing Bar. *Materials* **2023**, *16*, 2913. [CrossRef] [PubMed]
155. Xu, J.; Tan, Q.; Mei, Y. Corrosion protection of steel by Mg-Al layered double hydroxides in simulated concrete pore solution: Effect of SO_4^{2-}. *Corros. Sci.* **2020**, *163*, 108223. [CrossRef]
156. Wang, X.-H.; Xu, J.-X.; Tan, Q.-P. Effect of nitrite intercalated Mg−Al layered double hydroxides on mortar durability under Cl^- and SO_4^{2-}coexisting environment. *J. Cent. South Univ.* **2022**, *29*, 546–560. [CrossRef]
157. Chen, Y.X.; Shui, Z.H.; Chen, W.; Chen, G.W. Chloride binding of synthetic Ca–Al–NO_3 LDHs in hardened cement paste. *Constr. Build. Mater.* **2015**, *93*, 1051–1058. [CrossRef]
158. Wu, B.; Zuo, J.; Dong, B.; Xing, F.; Luo, C. Study on the affinity sequence between inhibitor ions and chloride ions in MgAl layer double hydroxides and their effects on corrosion protection for carbon steel. *Appl. Clay Sci.* **2019**, *180*, 105181. [CrossRef]
159. Yang, Z.; Polder, R.; Mol, J.M.C.; Andrade, C. The effect of two types of modified Mg-Al hydrotalcites on reinforcement corrosion in cement mortar. *Cem. Concr. Res.* **2017**, *100*, 186–202. [CrossRef]
160. Yang, Z.; Fischer, H.; Polder, R. Laboratory investigation of the influence of two types of modified hydrotalcites on chloride ingress into cement mortar. *Cem. Concr. Compos.* **2015**, *58*, 105–113. [CrossRef]
161. Cao, Y.; Zheng, D.; Dong, S.; Zhang, F.; Lin, J.; Wang, C.; Lin, C. A composite corrosion inhibitor of mgal layered double hydroxides co-intercalated with hydroxide and organic anions for carbon steel in simulated carbonated concrete pore solutions. *J. Electrochem. Soc.* **2019**, *166*, C3106. [CrossRef]
162. Zhou, P.; Xu, J.; Yu, L. Inhibitive effect of SiO_2@ NO^{2-} intercalated MgAl-LDH nanocomposite on steel in Cl^- contaminated saturated $Ca(OH)_2$ solution. *Corros. Sci.* **2022**, *195*, 109997. [CrossRef]
163. Wang, X.; Xu, J.; Ma, G. Hierarchical zeolite-LTA@Mg-Al layered double hydroxide core@shell structure with enhanced corrosion protection of steel in saturated $Ca(OH)_2$ solution. *J. Taiwan Inst. Chem. Eng.* **2021**, *122*, 260–272. [CrossRef]